Politecnico di Torino

Politecnico di Torino

Department of Environment, Land, and Infrastructure Engineering

Master of Science in Petroleum Engineering

A. y. 2023/2024

Well cementation processes in CO_2 storage activities

Supervisor:

Prof. ROMAGNOLI RAFFAELE

Candidate:

Sayed Ahmed Eslam Elaraby Rashad Mohamed

This page was intentionally left blank.

Abstract

At the global level, we are pretty much familiar with the scale of Co_x and NO_x pollutants rising rapidly year after year from various sources like industrialization, urbanization, and new technology production enhancement.

one of the major sources, no doubt is oil and gas production. Every year approximately $5.1\ million\ tons$ of CO_2 are produced from the production extraction and transport of oil and gas [41].

CO_2 injection into the reservoir at the subsurface level is one of the most efficient and reliable approaches to reducing CO_2 produced globally. but the normal cementation has an adverse effect on well stability. This thesis addresses the most methodical cementing approach for CO_2 injection. This research reports simulation results of super critical CO_2 effect on a cement sphere, the change of porosity, and the permeability over time. The simulation also addresses the diffusion of CO_2 into the matrix of standard Portland cement. Furthermore, it has mentioned the corrosion resistant material can be added to inhibit the act of carbonization and formation of carbonic acid such pozzolanic material, basalt ash, ACA, and nanoparticles filling the matrix of the cement.

Acknowledgement

I would like to thank Professor ROMAGNOLI RAFFAELE for his generous support. I also want to thank Politecnico di Torino and the department committee for their dedication and hard work. I also feel incredibly grateful for my friends and family for their endless support.

To my family Aamn, Esraa, Soso, Elaraby.

Table of contents

List of Figures

List of tables

1 Overview Cementing methodology.

Cementing a well is defined as the process of introducing cement to the annular space between the well and the casing to achieve zonal isolation and further good bonding between the wellbore and the casing string [1]. Cementing the well-bore was first introduced during the early 20^{th} century by Union Oil Company of California in an oil well named (Hill no. 4) on 26^{th} of September 1905 [2] in which the water had been seeped above the casing shoe and became more common and available in 1917. After almost 40 years of the first cemented well, the API has adopted code $no.32$ for the cementing of the oil wells [1]. Figure 1 1 shows a schematic illustration of:

(a) how cement is placed into the annular space between casing and rock,

and (b) how a finished well looks after all the casings are cemented in place [10]

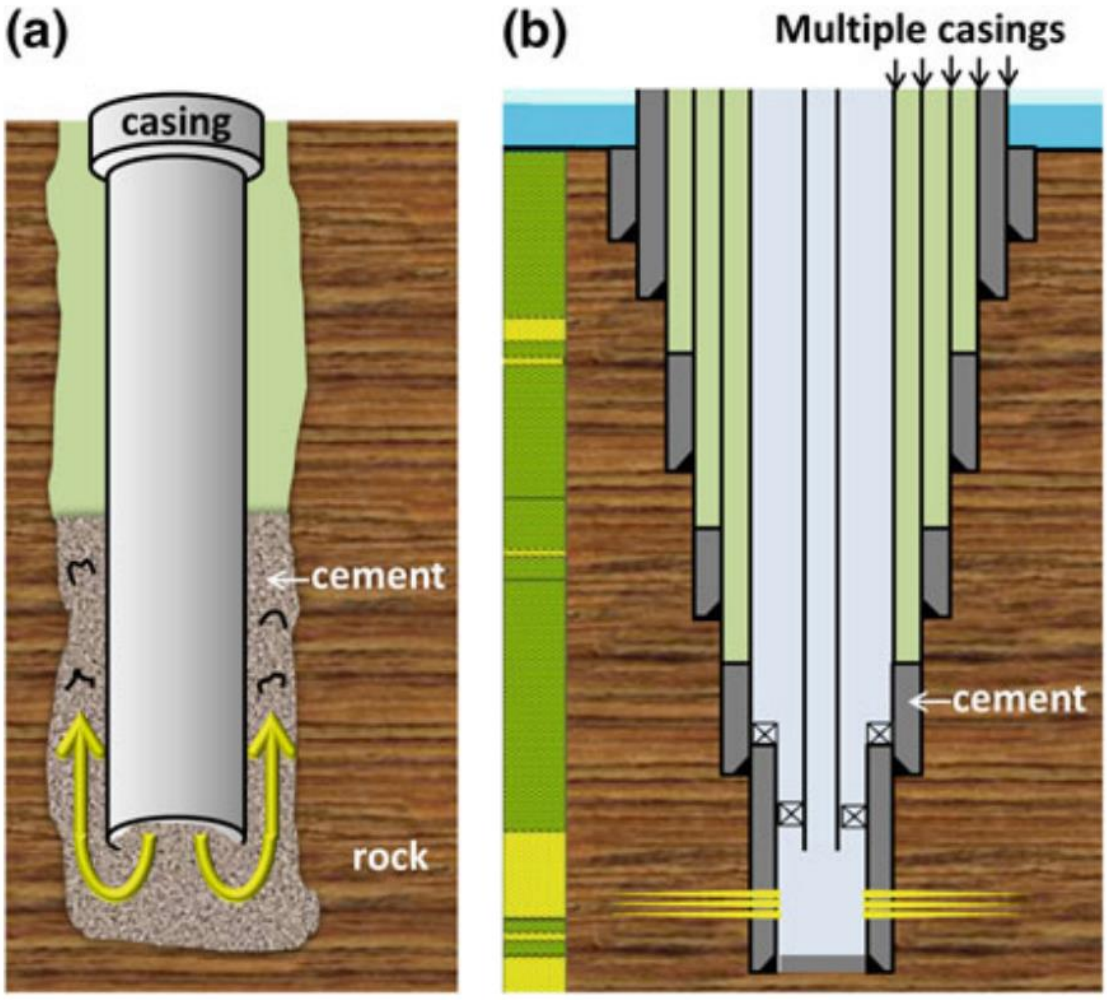

Figure 1-1 A schematic illustration of a how cement is placed into the annular space between casing and rock, and b how a finished well looks after all the casings are cemented in place [10]

1.1 Types of cementing

Cementing is subdivided into two categories: primary cementing and remedial cementing. Primary cementing is pumping cement into the well bore to provide zonal isolation, support axial load of casing sting, protect the casing from corrosion, provide stability to the wellbore. Portland cement is considered the most produced material of human life span, but the cement used in oil and gas is different from which used in construction. Additives must be added to the slurry pumped into the well to change the properties of it to coincide with the very specific condition of each well. Having a good cement job most likely to make the further drilling operations to be a success because if not remediation cementing is more difficult and not cheap at all for operating and also for not running time. Cementing is usually called one shot operation that must be planned well and operated with high experience and precision.

1.2 Cement chemical composition:

Portland cement is the key for modern construction, however cement used in the oil and gas industry is a modified version of it. The production of this cement is made from limestone and clay or shale at 1650 C and after that it enters a grinder that transforms it into a proper size. API has introduced 9 types of cement as shown in table 1-1 to be used in oil and gas fields which is based on the variation of pressure and temperature strength which is reflected by the depth of the well.

Table 1-1 Classification of different types of cement used in O&G. [4]

Class Type	Details
Class A	For use up to 6000 ft depth, when special properties are not required
Class B	For use up to 6000 ft depth, when conditions require moderate to high sulfate resistance.
Class C	For use up to $6000\ ft$ depth when conditions require high early strength.
Class D	For use from $6000\ ft\ to\ 10000\ ft$ depth, under conditions of high temperatures and pressures.
Class E	For use from $10000\ ft$ to $14000\ ft$ depth, under conditions of high temperatures and pressures.
Class F	For use from $10000\ ft$ to $14000\ ft$ depth, under conditions of extremely high temperatures and pressures.

Class G	Intended for use as a basic cement from surface to $8000\ ft$ depth Can be used with accelerators and retarders to cover a wide range of well depths and Temperatures.
Class H	A basic cement for use from surface to $8000\ ft$ depth as manufactured. Can be used with accelerators and retarders to cover a wider range of well depths and temperatures
Class J	Intended for use as manufactured from $12000\ ft$ to $16000\ ft$ depth under conditions of extremely high temperatures and pressures. It can be used with accelerators and retarders to cover a range of well depths and temperatures.

This version of Portland cement is made up from four compounds:

Table 1-2 Component of Portland Cement [5][1]

Oxide Composition	Cement Notation	Concentration	Common Name
$3CaO.SiO_2$	C_3S	$55-65$	Alite
$2CaO.SiO_2$	C_2S	$15-25$	Belite
$3CaO.Al_2O_3$	C_3A	$8-14$	Aluminate
$4CaO.Al_2O_3.Fe_2O_3$	C_4AF	$8-12$	Ferrite Phase

The rheological properties are mainly dominant by the C_3A and C_4AF, but the other two compound C_3S and C_2S are controlling the mechanical strength of the cement.

While mixing water with cement, C_3S and C_2S form a calcium silicate hydrates gel ($C-S-H.$) and calcium hydroxide $C-H$.

1.3 Reactions:

$$2C_3S+6H\ \rightarrow C-S-H+3CH$$

$$2C_2S+4H\ \rightarrow C-S-H+CH$$

1.4 Density:

Meanwhile, in the drilling process and design, the most predominant parameters are to determine the pore pressure and fracture pressure. We can define pore pressure as the pressure of fluids within the formation, Fracture pressure is the maximum pressure after

which the formation can be fractured, and we may encounter loss of circulation. The pore pressure threshold is almost $0.433\ psi/ft$ Psi/ft depth above which we are in an abnormal pressure zone and vice versa. [4][6]

The density of cement defines the pressure of the hydrostatic column in the well pore that must be above pore pressure to avoid have formation of fluid into the wellbore and below the fracture pressure to avoid the fracture of the formation. Neat Cement slurry has a density between $1.67\ to\ 2.15\ g/cm^3$. The density is a factor that can be increased or decreased by some additives and is dominated by Cement to water ratio. Densified cement ranges between $1.91\ to\ 2.39\ g/cm^3$ and water-to-cement ratio slurries have a density of $1.31\ to\ 1.8\ g/cm^3$. [4][7][8]

1.5 Rheology of cement

While Cement in a slurry state it is predominant by its rheological state such as: Yield stress and plastic viscosity. Yield stress is the minimum stress required for a non-Newtonian fluid to start to flow. There are multiple models to describe the relation between the shear stress: $\boldsymbol{\tau\ (Pa)}$ and shear rate $\boldsymbol{\dot{\gamma}\ (s^{-1})}$. The Bingham model as shown in figure 1-2 represents the shear stress is a linear function of the shear rate with Y-intersect of yield stress $\boldsymbol{\tau_Y\ (Pa)}$ and slope of plastic viscosity $\boldsymbol{\mu_{pl}\ (Pa\ .s)}$.

$$\tau = \tau_Y + \mu_{pl}|\dot{\gamma}|$$

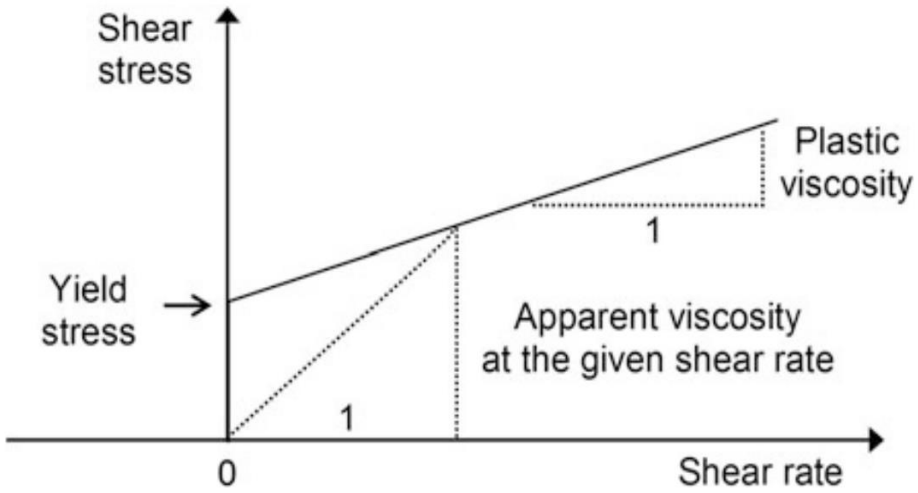

Figure 1-2 Shear stress Vs. shear rate in Bingham model [10]

For normal Newtonian fluids, the graph starts from point zero with $\boldsymbol{\tau_Y = 0}$ [10][4].

Another model can be introduced for developing the Bingham model that the relation between shear stress and shear rate is not linear and the slope of the graph: Shear stress Vs. The shear rate is the apparent viscosity.

$$\tau = k\,\dot{\gamma}^{n}$$

While k is the consistency n is the power law exponent and τ shear stress $\dot{\gamma}$ is the shear rate. The exponent n defines the fluid as shear thinning or shear thickening. [9]

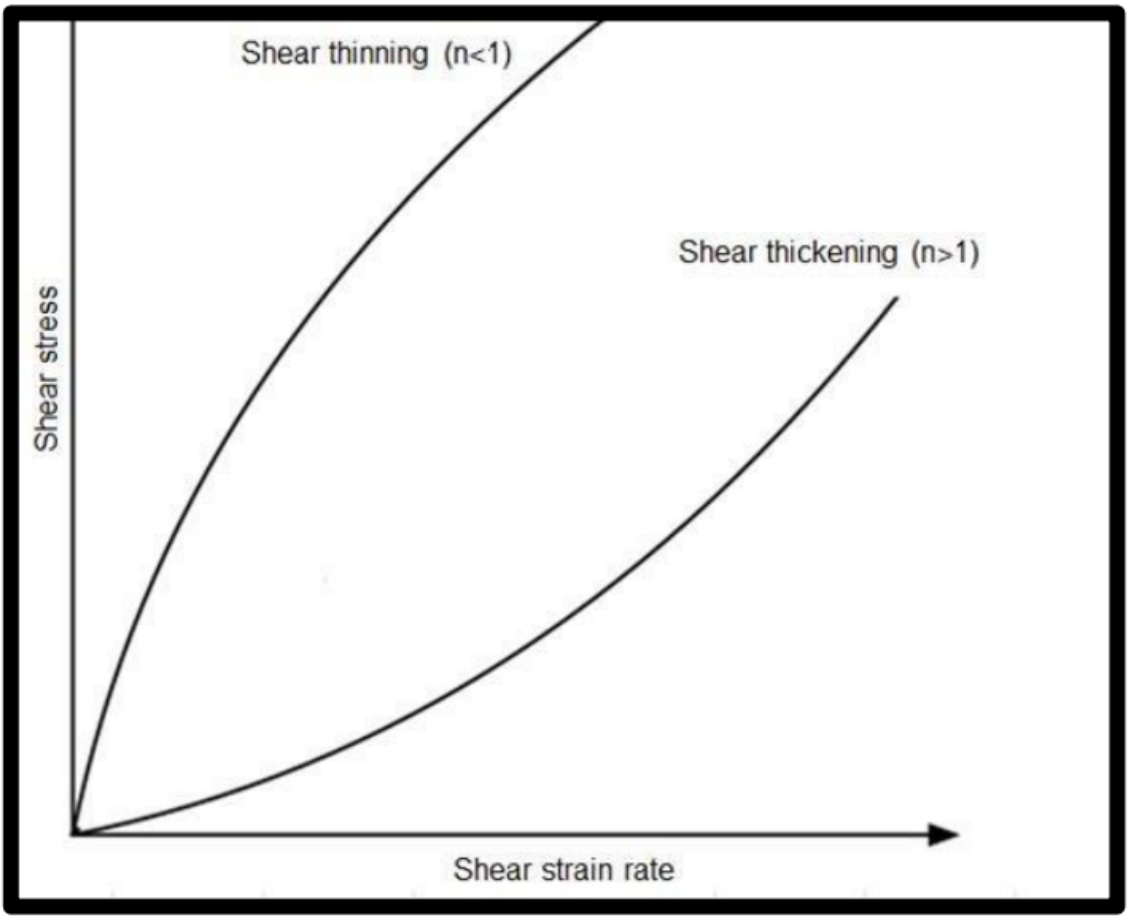

Figure 1-3 Power-law fluid model representation [9]

Further, the development of both models is the Herschel-Bulkley model in which both models are combined with the initial shear required for starting to flow. [2]

$$\tau = \tau_0 + k\,\dot{\gamma}^{n}$$

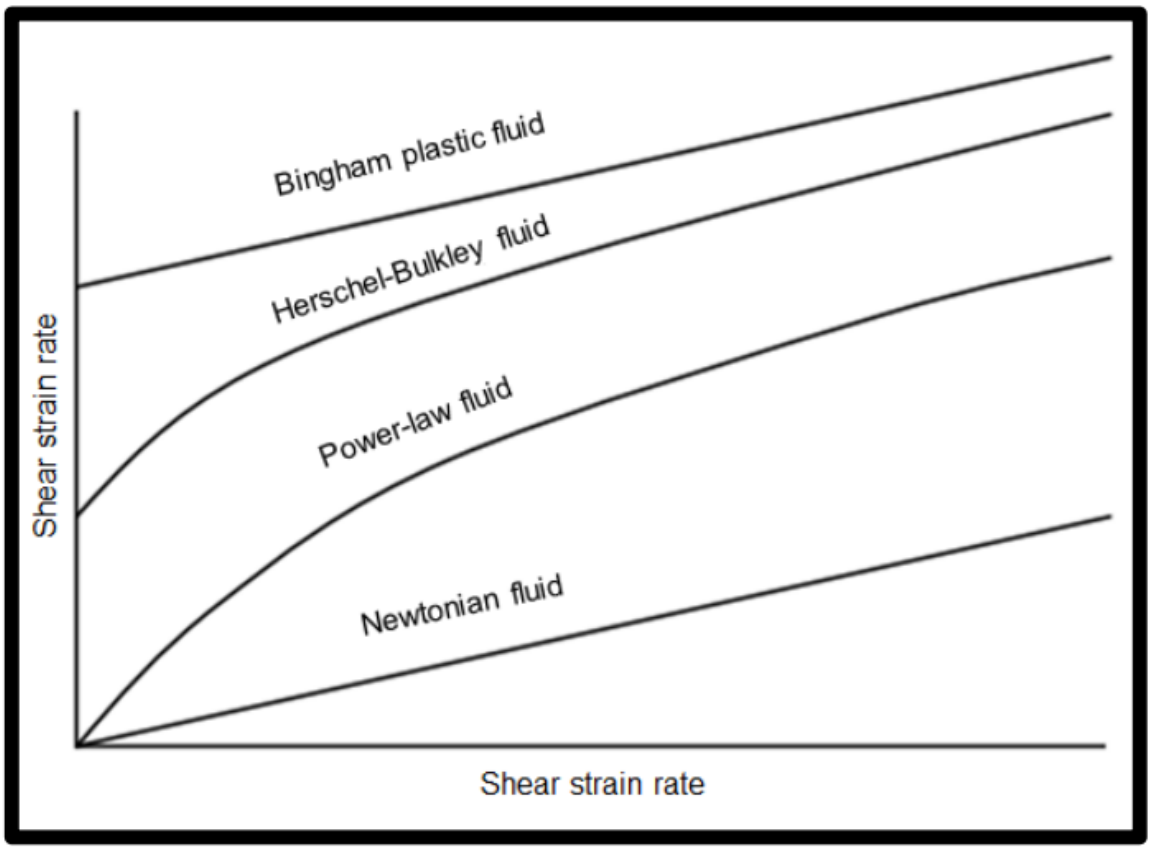

Figure 1-4 Newtonian and different non-Newtonian fluids behaviors. [2]

Studying the rheological properties of Cement for oil and gas is more complicated for other operations due to the high pressure and temperature state in the wellbore. these parameters are critical because the changes in rheological properties can affect the pumpability and flowability. [11]

1.6 Fluid loss

The leakage of water in cement slurry can occur while pumping the cement into the annulus due to the difference between pore pressure and the cement hydrostatic pressure. Fractures in the formation and high permeable layers encounter dehydration of the cement slurry which is called filter cake, and it affects the water in cement ratio and hence the properties of the flurry such as the hydrostatic pressure. This phenomenon affects the quality of isolation of the formation and may have seepage of formation fluids into the wellbore. [12][13][14]

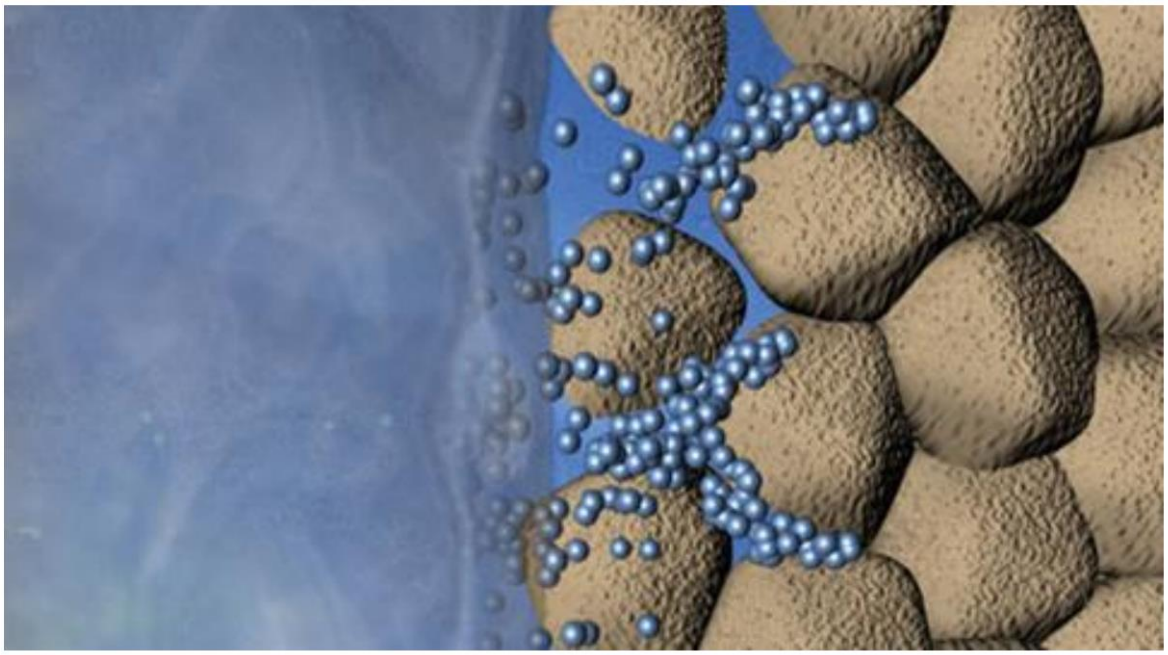

Figure 1-5 Fluid loss scheme [1].

1.7 Mechanical properties

Cement is subjected to many stresses in the well bore that has to withstand and provide stability. in case the stress applied to the cement goes over its mechanical strength micro fractures are likely to develop in the cement sheath and lose the zonal isolation property. the remediation process for fractured cement is expensive and lack of success will force the well to shut in. [15][16]

to evaluate the mechanical properties of cement, a sample of the hardened sheet is taken into the laboratory to measure its compressive strength and more research has proven that it is enough for a good evaluation of the cement properties as it has to take into consideration more properties like young's modules, Poisson ratio, and tensile strength.[17][18]

- Factors affecting the mechanical properties of hardened cement:

Temperature: with high temperature the process of dehydration of the cement which in return increases its compressive strength.

pressure: Lower compressive strength happens with increasing the pressure on the cement slurry as it increases the setting time. However, it is not consistent like the temperature effect.

Water content: the mechanical strength is lower in case of increasing the water to cement ratio.

1.8 thickening time

thickening time is the time required for the cement slurry to start hydration and transform from liquid state to solid state, in other words, it is the duration that the cement slurry can be pumped into the well bore before solidification. thickening time depends on mostly pressure and temperature, additives are introduced to affect the thickening time modification. [19][20]

1.9 Cement additives

Cement is mixed with additives to modify its rheological and mechanical properties to allow placement of cement in different conditions with high efficiency. [1][2].

1.9.1 Accelerators:

Accelerators are chemicals that are responsible for decreasing thickening time of a slurry and increase the rate of early strength development [33]. Wells in shallow depth are required to add accelerators to reduce the Wait-on cement time and save the highly expensive rig time.[36] The most common accelerators are salts like Calcium chloride $\boldsymbol{CaCl_2}$ and sodium chloride $\boldsymbol{NaCl}$. Calculating thickening time is crucial and has to be with a good margin in case of emergency shutdown [2]. Table 1-3 shows the maximum concentration of accelerators, by the unit by weight on cement percent, above which the opposite reaction is most likely to happen [37][36].

Table 1-3 The recommended concentrations of accelerators. [37]

	Maximum concentration ($\%\ bwoc$)	Temperature °$\boldsymbol{C}$
$\boldsymbol{CaCl_2}$	$1.5 - 2$	$4 - 49$
$\boldsymbol{NaCl}$	$2 - 2.5$	< 70

1.9.2 Retarders

Retarders are chemicals used for increasing the thickening time which gives the operator more time for any unexpected events. The temperature has a great effect on Retarders as the behavior of the slurry with Retarders is different on the surface with the same slurry in the borehole especially in high-temperature bottom-hole. [2][1] Each retard has a range of operating temperatures which can have a counter-effect on the thickening time in case of misuse.[34]. Shown in the figure the effect of adding retarder agent with increasing the temperature on the thickening time. [1]

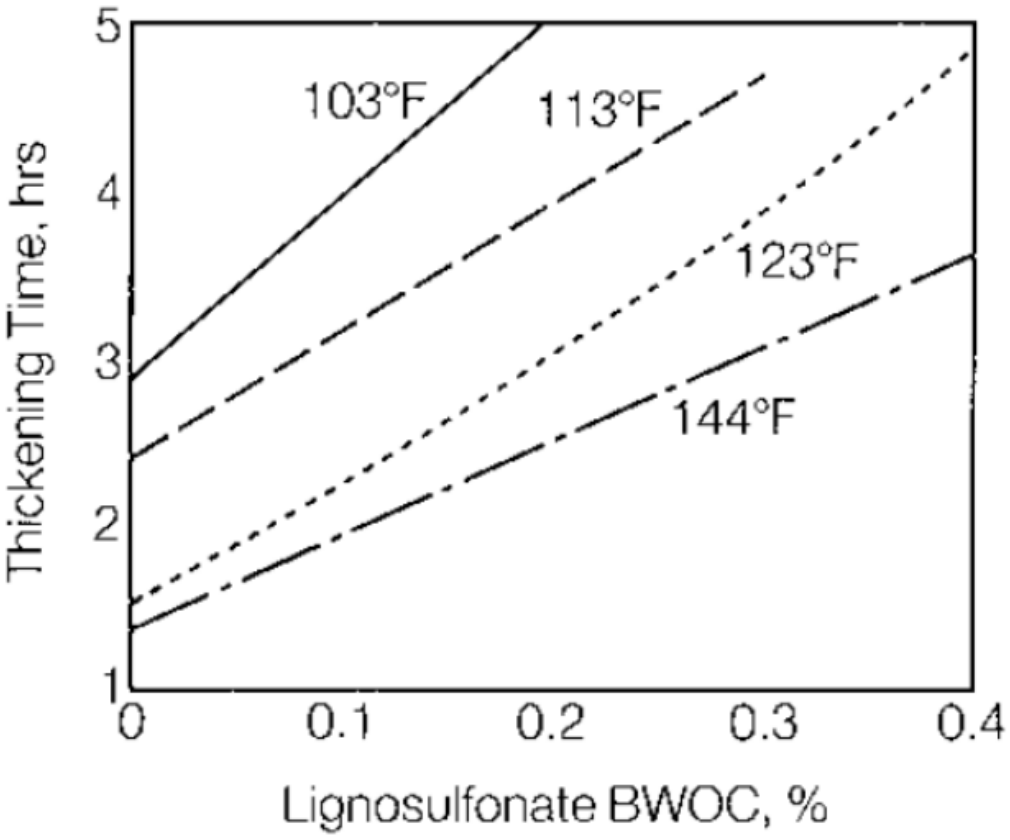

Figure 1-6 The effect of adding lignosulfonate as a retarder agent by different temperature [1]

1.9.3 Weighting agents

Weighting agents are used to increase the density of cement slurry. The most common Weighting agents are hematite and barite. Figure 1-6 shows the changing of slurry density in accordance with adding weighting agents [1]

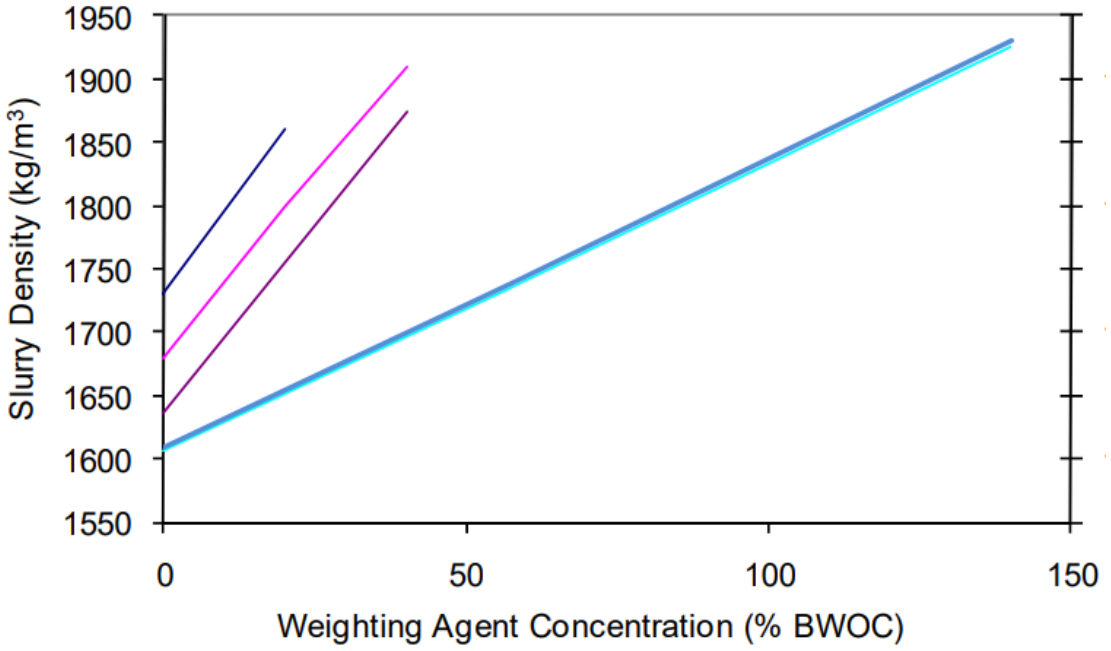

Figure 1-7 Relation between slurry density and concentration of weighting agents. [1]

1.9.4 Dispersants

Dispersants are used to reduce friction and increase mixability of the cement blending.

1.9.5 Extenders

Extenders are used to increase the volume of cement product for each sack used, thus decreasing the density of the system. They also affect the cement by the mean of decreasing the compression strength and the cost of the slurry many additives can be used as extenders such as bentonite, sodium silicate, and fly ash [34].

The mixture of cement is balanced for specific conditions in the wellbore and taken into consideration that each additive can react with each other. In the figure 1-6 and figure 1-7, It shows the effect of each additive relative to each other through time as a function of consistency and compression strength [34].

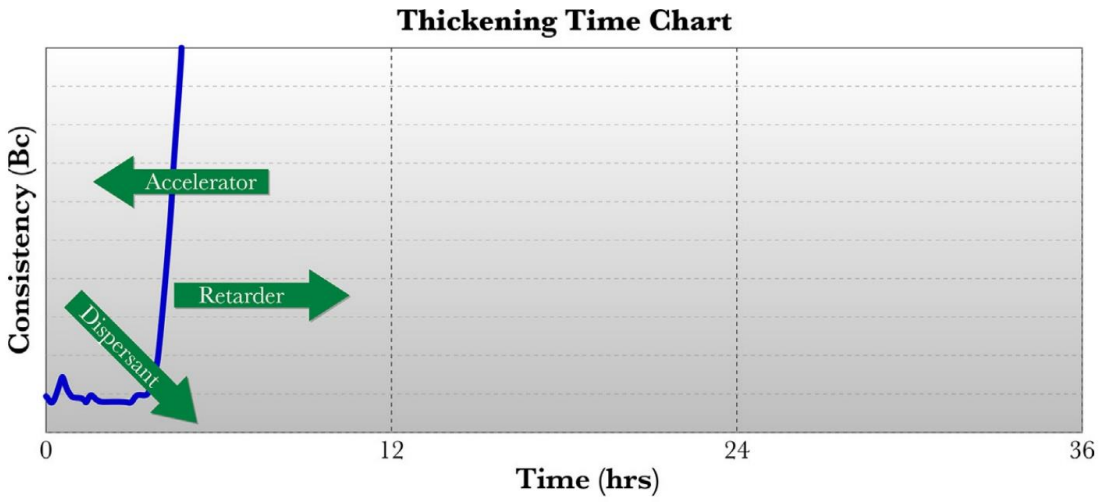

Figure 1-8 Interaction and effect of additives on consistency [34]

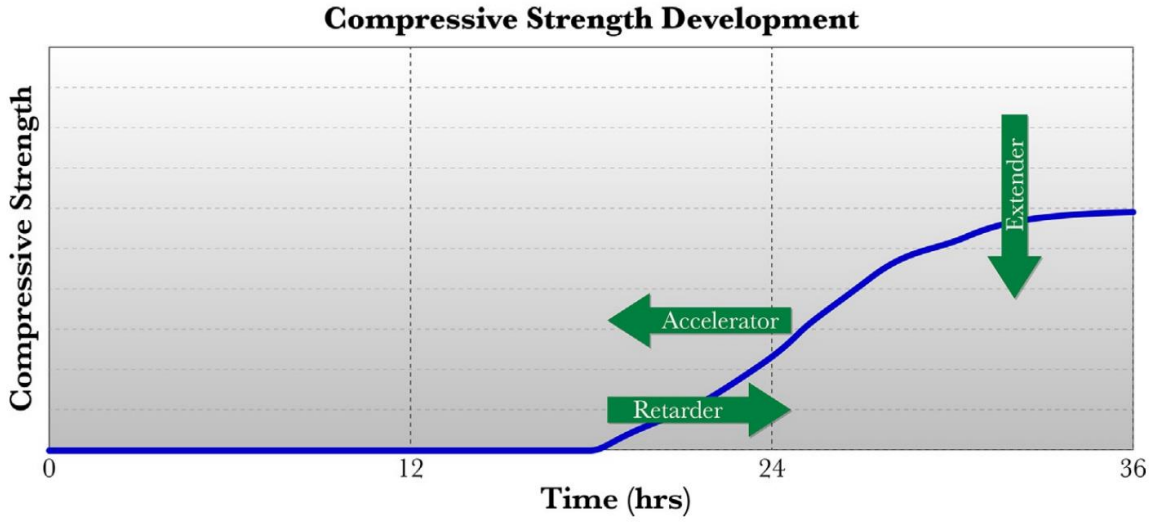

Figure 1-9 Interaction and effect of additives on compression strength [34]

In table 1-4, IADC Drilling Manual shows the effect of each common additive.

Table 1-4 Most common additive and their effect on the slurry [35]

✓ = Major Effect; ✗ = Minor Effect; [blank] = no or insignificant effect											
Additive Type or Effect → Cement Property Affected ↓	**Effect**	**Extenders (Bentonite, Pozzolans, etc.)**	**Accelerators**	**Retarders**	**Dispersants**	**Sand and silica flour**	**Free Water Control**	**LCM**	**Gas Migration Agents**	**Weighting Agents**	**Salt (NaCl)**
Density	Increase				✓	✓				✓	✗
	Decrease	✓									
Water Requirement	More	✓				✓		✗			
	Less				✓						
Viscosity	Higher	✗	✓			✗	✓				✗
	Lower			✗	✓					✓	✗
Thickening Time	Longer	✗		✓	✓		✓		✗		✓
	Shorter		✓								✓
Early Strength	More		✓								✗
	Less	✓		✓	✗		✗				✗
Ultimate Strength	More					✓					
	Less	✓									
Durability	Better	✓				✓			✗		
	Worse									✗	
Fluid Loss	Improved	✗	✗	✗	✓				✓		
	Worse										✗
Free Water	Less				✗				✓		
	More	✓			✓		✓				✗

2 Cement in CO_2 storage

According to the International Energy Agency (IEA), by 2050, 5 billion tons of CO_2 per year could be avoided through CO_2 capture and storage, representing a 16% contribution to the reduction of global greenhouse gas emissions [23]. Carbon Capture Storage is defined as a way of reducing carbon emissions by injecting CO_2 into a geological layer.[22] It was introduced that injecting CO_2 into an abandoned oil well can be achievable but it can face problems related to pre-cemented wells. Severe corrosive material found in presence of CO_2 in super critical state and dissolved in formation water can act a corrosive material that affects the cement and the casing which threaten the integrity of the wellbore. The formation of carbonic acid, Carbonation and Joule Thomson effect are mostly common phenomena that lower the compressive strength of cement and casing steel. [21]

2.1 Effect of $\boldsymbol{CO_2}$ injection to the cement:

2.1.1 The formation of carbonic acid

Supercritical CO_2 injection in the reservoir with high pressure and temperature behaves like more liquid than gas with higher viscosity and less volume.[24] CO_2 in such a state is more likely to dissolve in formation water and produce carbonic acid, which attacks the cement matrix, reaching the pores of cement containing water and the process is continuous to some extent in the cement column. The presence of carbonic acid lowers the pH value, and partial pressure of CO_2 and other ions in the cement converting $Ca(OH)_2$into $Ca^{+2}$and $2OH^-$ as shown in the figure 2-1.

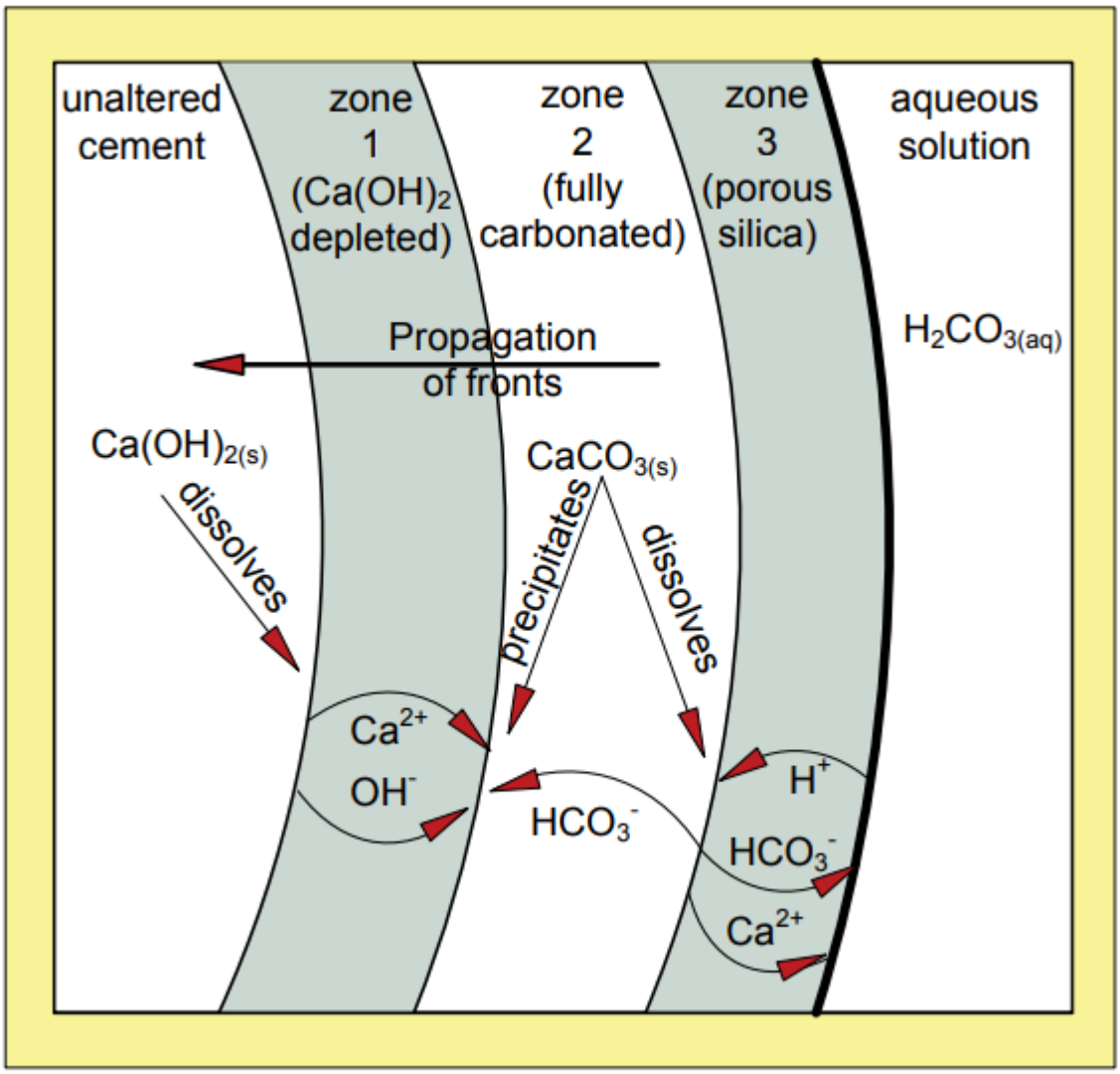

Figure 2-1 Attack of carbonic acid to the cement. [25]

2.1.2 Carbonation

Furthermore, attacking the cement layer, Carbonation is the formation of calcium carbonate in the mean of two important materials in the cement installed in the well bore: calcium hydroxide and calcium silicate hydrates by the following corrosive reactions [26]:

$$Ca(OH)_{2(aq)} + CO_{2(aq)} \rightarrow CaCO_3 + H_2O$$

$$C_xSH_y + x\ CO_{2(aq)} \rightarrow x\ CaCO_3 + SiO_2\ .y\ H_2O$$

The first equation describes the carbonation of calcium hydroxide into calcium carbonate. Once it is all consumed the second reaction is taking place to convert the Calcium silicate hydrate into calcium hydroxide and silica gel as illustrated in Fig2-2 [26] [27]. Super critical

carbon dioxide is considered the more severe effect int the vicinity of the wellbore. [28] according to Nedljka research paper these processes causes densification leading to increased hardness and decrease permeability, hence it has an extreme effect on production of micro and even macro fracture into the cement matrix.[23] Trough the propagation of the carbonation, the speed of the process decreases with time because of the precipitation of calcite into the cement sheath [30]. However, it can be beneficial for the cement to reduce the permeability but in severe cases it could make the cement lose its integrity. [29]

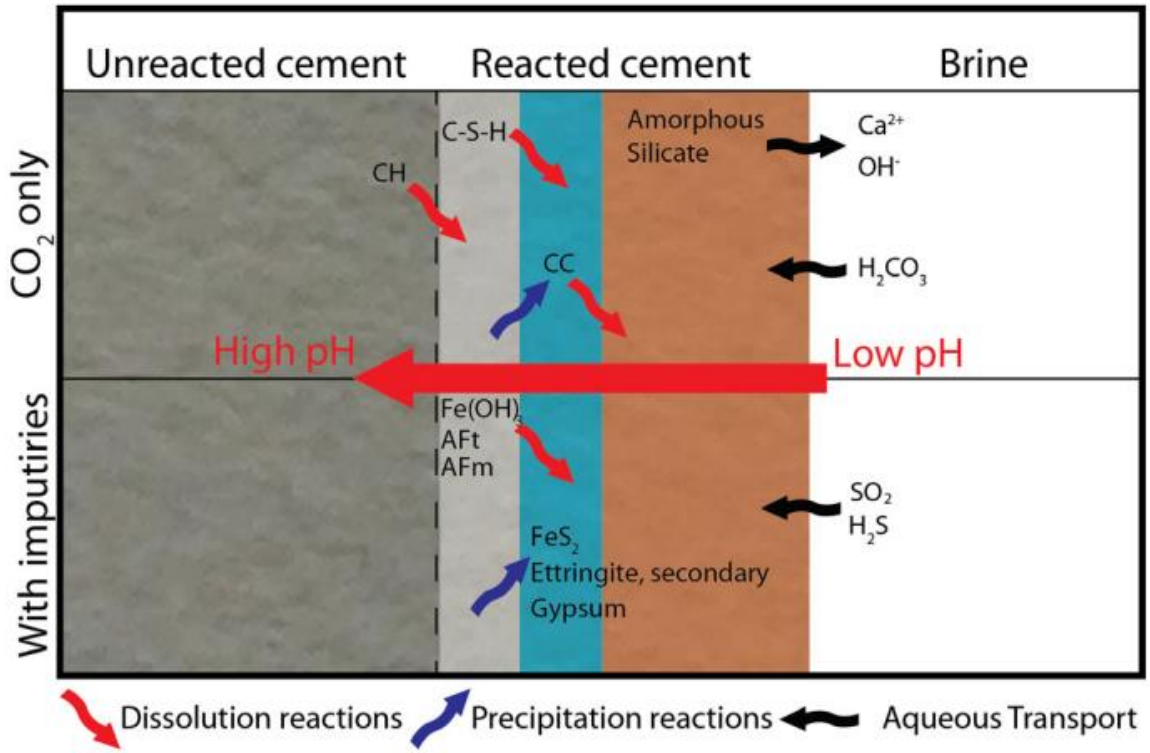

Figure 2-2 Schematic interaction between well cement and CO_2 [31]

2.1.3 Bi-Carbonation

Most oil reservoirs filled with saline water which can be saturated with super critical carbon dioxide can transform calcium carbonate into calcium bicarbonate as shown in the equation [23].

$$CaCO_3 + H_2CO_3 \rightarrow Ca(HCO_3)_2$$

The ability to calcium bicarbonate to dissolve into water is very high and it will leave the cement matrix behind resulting in increasing porosity and hence the permeability of the cement sheath [32].

3 Simulation study of carbonation effect

This contribution was cited from the work of Jena Jeong et al studying the carbonation process and simulation for cement in highly CO_2 corrosive medium.

3.1 The upper limit of CO_2 calculation:

The modeling of carbonation process for calculating CO_2 uptake engage with the surface which has a direct contact with the injected CO_2, carbonation depth, diffusion of CO_2, the interconnect porosity and the conditions while which the process happens, however it does not take into account the hydration reaction during the phase of carbonation. The calculation for CO_2 uptake for early phase was estimated by Steinour: [42]

$$CO_2 uptake(\%) = 0.785 \times (CaO - 0.7SO_3) + 1.091 \times MgO + 1.420\, Na_2O + 0.935\, K_2O$$

The mentioned formula indicates an overestimation of CO_2 consumed during the carbonation in standard conditions of $101.325kPa$ of pressure. This formula does not take into account the kinetic reaction for CO_2, content of water, temperature or concentration of CO_2 however it provides the maximum value of CO_2 reaction with the component of cement. It is considered as the limit of CO_2 consumption for the model established to simulate CO_2 effect on cement compounds [46].

3.2 Multi-reactive carbonation model:

In the progress of developing the model, it was added to the model the multi-reactive carbonation as it takes into account hydrate and anhydrate minerals [43][44]. It was observed that hydration of cement and carbonation can happen at the same time although the fact that carbonation produces water in this model as the components CSH, $Ca(OH_2)$, C_2S and C_3S react with CO_2 concurrently

The equations that describe the process: [46]

$$3CaO.2SiO_2.3H_2O + 3CO_2 \xrightarrow{r_{CSH}} 3CaCO_3.2SiO_2.3H_2O$$

$$Ca(OH_2) \overset{r_D}{\leftrightarrow} Ca^{2+}_{aq} + 2OH^-_{aq}$$

$$Ca^{2+}_{aq} + 2OH^-_{aq} + CO_{2(g)} \overset{r_{CH}}{\longleftrightarrow} CaCO_{3(s)} + H_2O$$

$$3CaO.SiO_2 + 3CO_2 + vH_2O \xrightarrow{r_{C_3S}} SiO_2.vH_2O + 3CaCO_3$$

$$2CaO.SiO_2 + 2CO_2 + vH_2O \xrightarrow{r_{C_2S}} SiO_2.vH_2O + 2CaCO_3$$

In the last two equations, Anhydrous carbonation is viable theoretically as it was tested by spectroscopy [47].

Reaction rates can be calculated as:

$$r_{CSH} = k_{CSH} a_s [CSH] V_{CSH} [CO_2]$$

$$r_D = 0.5\, f_w k_s a_s \left[Ca(OH)_{2(s)}\right] \bar{V}_{CH} \left([OH^-]_{eq} - [OH^-]\right)$$

Where:

f_w : volume fraction of aqueous film,

k_s : mass transfer coefficient for the dissolution of $Ca(OH)_{2(s)}$

a_s : specific surface area of concrete pores in contact with water,

$\left[Ca(OH)_{2(s)}\right]$: molar concentration of $Ca(OH)_{2(s)}$

$[OH^-]_{eq}$: molar concentration of OH^-_{eq} in the aqueous phase of the pores in equilibrium or saturation state

$[OH^-]$: molar concentration of OH^-in the aqueous phase of the pores.

$$r_{CH} = HRTk_2[OH^-]_{eq}[CO_2]$$

H : Henry's constant for the dissolution of CO_2 in water,

R : gas constant,

T : absolute temperature in Kelvin

k_2 : constant rate for CO_2 and OH–

$$r_{c_3S} = k_{C_3S}a_s[C_3S]\bar{V}_{C_3S}[CO_2]$$

$$r_{c_2S} = k_{C_2S}a_s[C_2S]\bar{V}_{C_2S}[CO_2]$$

Equations for CSH, C_3S and C_2S reaction rates can be shortened to:

$$r_j = k_j a_s[j]\bar{V}_j[CO_2]\ for\ j = CSH, C_3S, C_2S$$

Where:

$[j]$: the molar concentration of constituent j (in moles per unit volume of concrete),

k_j : rate constant for the reaction of constituent j with CO_2,

a_s : specific surface area of concrete pores in contact with water,

$\bar{V}_j$: the molar volume of constituent j and CO_2 molar concentration.

The reaction rates in Equations are taken into account to assess CO_2 consumption rate in the sink term of CO_2 gas diffusion equation by applying mass balance equation:

To calculate CO_2 consumption, equations of r_{CSH}, r_{C_3S}, r_{C_2S} can be used in sink term in the mass balance equation:

$$\frac{\partial(P(t)(1-f)[CO_2]}{\partial t} = \left(-Div\left(-D_{e,CO_2}\nabla[CO_2]\right)\right)_{Diffusive\ term}$$

$$-\left(P_0 f_w r_{CH} - 3r_{CSH} - 3r_{C_3S} - 2r_{C_2S}\right)_{Sink\ term}$$

$$Where\ D_{e,CO_2} \approx 1.68\ \times 10^{-6}(P_P(t)^{1.8}\left(1-\frac{RH}{100}\right)^{2.2}$$

Where:

$P(t)$: The current porosity is considered for CO_2 diffusion based on the initial porosity P_0

D_{e,CO_2} : signifies an effective diffusivity as a function of hardened cement paste $P_P(t)$

RH : relative humidity

The carbonation equations for the model, by applying mass balance can be modified into:

$$\frac{\partial[CSH]}{\partial t} = -r_{CSH} + r_{H,CSH}$$

$$\frac{\partial[Ca(OH)_{2(s)}]}{\partial t} = -r_{H,CH} + r_D$$

$$\frac{\partial\left(P(t)\left[Ca(OH)_{2(aq)}\right]\right)}{\partial t} = -Div\left(-D_{e,\left[Ca(OH)_{2(aq)}\right]}\nabla\left[Ca(OH)_{2(aq)}\right]\right) - (P_0 f_w r_{CH} - r_D)$$

$$\frac{\partial[C_3S]}{\partial t} = -r_{C_3S} + r_{H,C_3S}$$

$$\frac{\partial[C_2S]}{\partial t} = -r_{C_2S} + r_{H,C_2S}$$

As mentioned, determining the total amount of CO_2 that has reacted with the cement components during the 14-day carbonation period is of great interest in cement and concrete research. The total quantity of CO_2 that has reacted with cement components in the numerical specimen can be calculated by double integrating the sink term over the volume and time domains where the sink term accounts for the consumption of CO_2 due to the chemical reactions with cement components during the carbonation process. This is achieved through a double integral over the volume and time, expressed as:

$$m_{CO_2} = \int_0^{t_0}\int_{\Omega\subset\mathbb{R}^3}(P_0 f_w r_{CH} - 3r_{CSH} - 3r_{C_3S} - 2r_{C_2S})\,d\Omega dt$$

Where:

m_{CO_2} is the total mass of CO_2 reacted with cement components.

t_0 is time at the end of carbonation simulation.

We divide the total mass of CO_2 reacted with the cement components, m_{CO_2} by total mass of specimen before carbonation tests and we define total amount of CO_2 sequestration in mass percent:

$$CO_{2_{seqeuestration}} = \frac{m_{CO_2}}{m_{specimen}} = \frac{\int_0^{t_0} \int_{\Omega \subset \mathbb{R}^3} (P_0 f_w r_{CH} - 3r_{CSH} - 3r_{C_3S} - 2r_{C_2S})\, d\Omega dt}{\int_{\Omega \subset \mathbb{R}^3} \rho_{specimen}\, d\Omega} \times 100$$

Where:

$m_{specimen}$ is the mass of specimens.

$\rho_{specimen}$ is the density before carbonation experiments.

3.3 Simulation results:

multi-reactive carbonation modelling was used to calculate the uptake of CO_2 possessed by the samples which is made of homogenous concrete aggregates. Consequently, it is mandatory to calculate the reliability and efficiency of the model on homogenous concrete aggregates by single phase in addition to two phase concrete. In the subsequent sections it provides two numerical simulations with the solutions of an extremely nonlinear transient system of partial differential equations as provided earlier. The simulation results give detailed about diffusion of CO_2 sequestration and compared with experiments results to have an analysis between both scenarios. [46]

- Single phase simulation

The customized COMSOL code was applied to the software with partial differential equations system of reactive transport modelling which was numerically computed employing the finite element method [46][48][49]. To facilitate an accurate comparison with the experimental observations all simulation used CO_2 concentration of $15\ vol\%$ is used. Plots and snapshots are provided below for the single-phase carbonation of $1, 2, 3, 7, and\ 14$ days and also the experimental data. It was assumed that the cement aggregate can be approximated as a sphere particle with a diameter of 40mm.

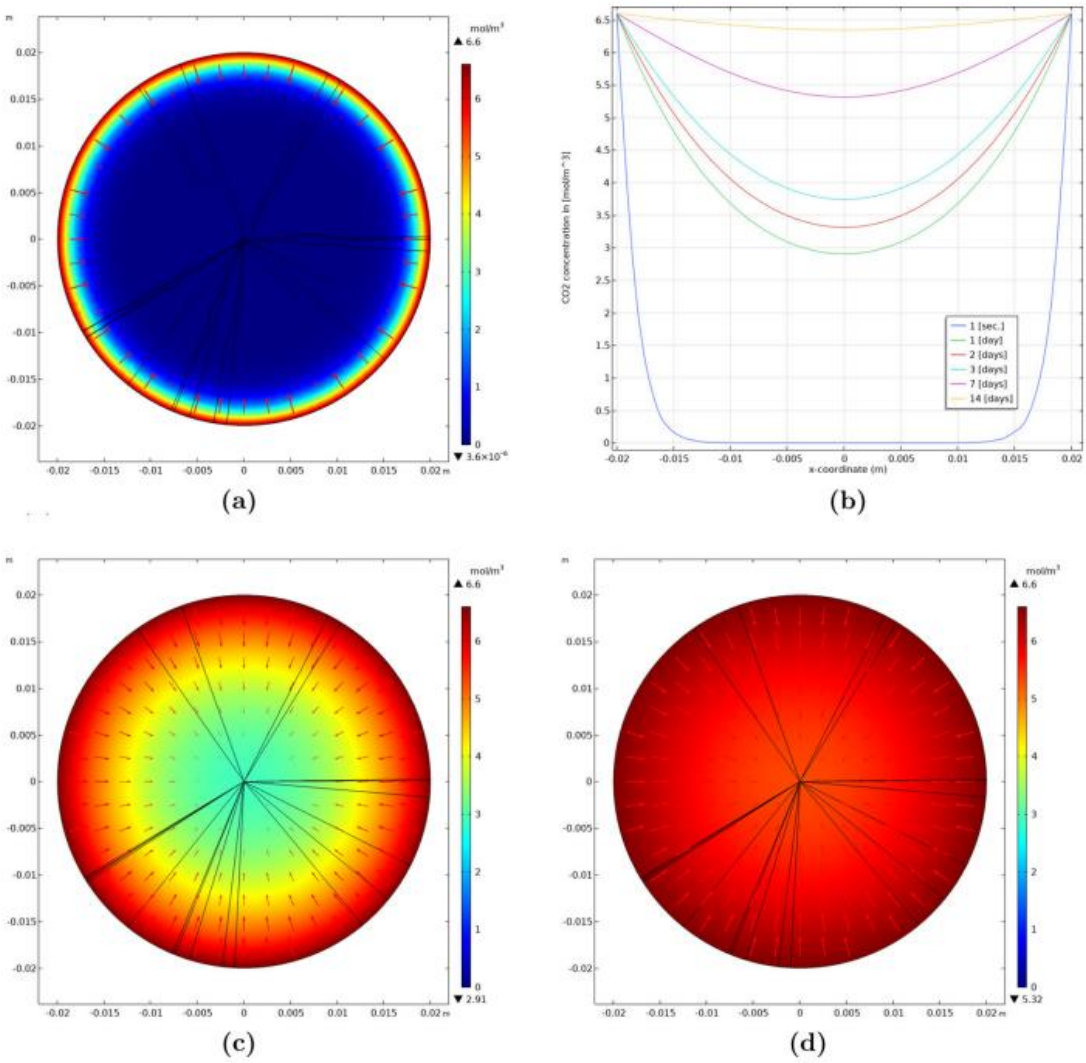

Figure 3-1 Simulation results CO_2 diffusion in single phase model from [46]

In Figure 3-1:

Section (a), a 2D-slice of our 3D carbonation model is shown highlighting the CO_2 concentration distribution with flux vector-field marked as red arrows.

Section (b), CO_2 concentration versus diameter is plotted sides deal with the external surfaces and middle point indicates the center of sphere. we note that CO_2 diffusion is very quick at the first day of carbonation and subsequently, we arrive at 7 $Vol\%$ of CO_2 concentration at the centre of spherical specimen [59]. The carbonation concentration reaches nearly 10 $VoI\%$ of CO_2 concentration at 7 days of carbonation in the centre of specimen. After 14 days of carbonation, 15 $Vol\%$ of CO_2 concentration can be observed in the whole specimen.

Section (c, d): it is the visual distribution of CO_2 into the cement sphere at 1 day and 7 days.

We focus on the cement components consumption during the carbonation process $Ca(OH)_2$ and CSH is consumed. These hydrate products are consumed very fast at the left

and right sides (external surfaces of our spherical specimen). At the end of 14 days of carbonation, these products have nearly vanished [55][56][57][58]

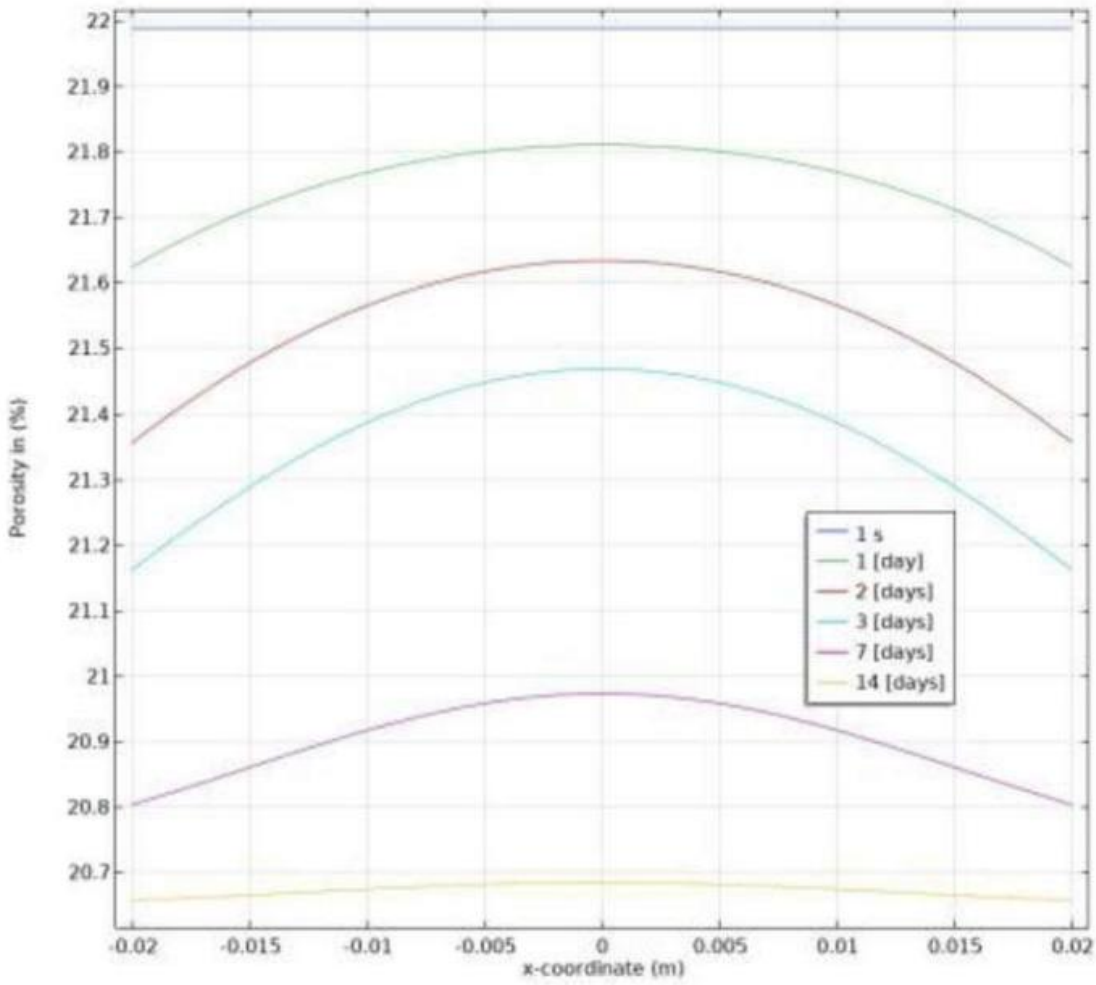

Figure 3-2 Porosity distribution in the specimen [46]

In Figure 3-2, the porosity change due to chemical reaction during carbonation process is illustrated. the initial porosity 22% is rapidly reduced on the left and right surfaces, showing the effect of CO_2 carbonation. After 14 days of carbonation, the chemically induced porosity is nearly 20% throughout the entire specimen, as reported in references [50]-[54]. It is important to note that the porosity distribution shown in Figure accounts only for the changes due to chemical reactions during carbonation and does not consider the additional porosity changes resulting from carbonation shrinkage and moisture transfer in the porous media, as discussed in references [46], [65], and [66]. In fact, the total porosity change must be significantly greater than the chemically induced porosity presented here [60]. The mechanical aspects stemming from carbonation shrinkage have been previously studied using micro-dilatation theory and Cosserat theory [46][59].

- Two phase simulation

In this part, we investigate a two-phase carbonation simulation model. The same CO_2 concentration of 15 $Vol\%$ is applied for the carbonation simulation as before. Once again, the concrete aggregate is assumed to be a spherical particle with a diameter of 40 mm. We construct this spherical specimen containing spherical aggregate inclusions within. To generate a realistic two-phase concrete aggregate model, we employ a user-written spherical packing algorithm implemented in MATLAB-COMSOL. This algorithm randomly computes the positions and radii of the spherical aggregate inclusions. Additionally, it allows us to approximately simulate the granulometry curve (particle size distribution) of the actual concrete aggregate specimens used in experiments.

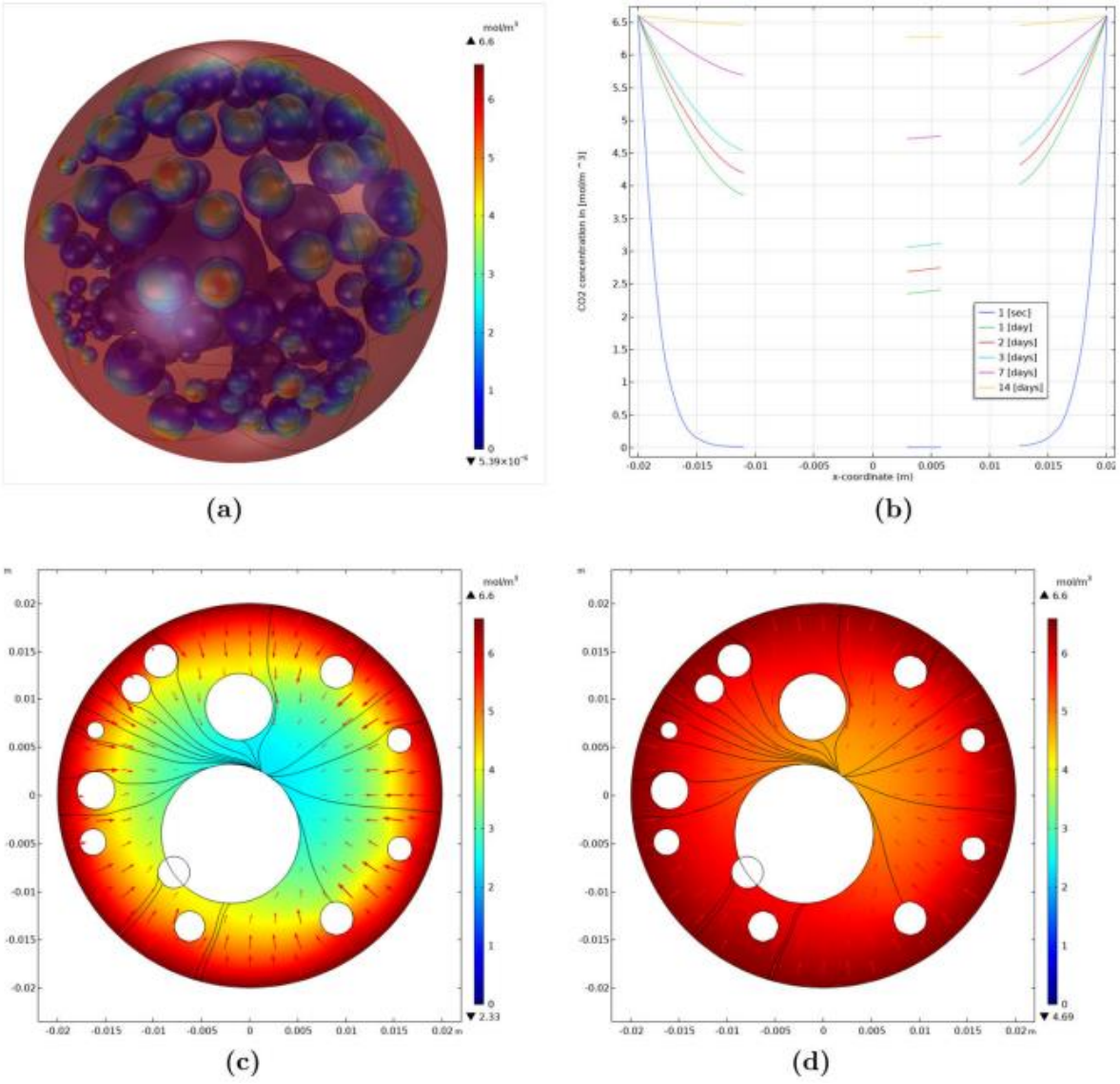

Figure 3-3 Simulation results CO_2 diffusion in two phase model from [46]

Figure 3-3 illustrates the CO_2 diffusion profiles in the two-phase model. These results are obtained from solving the partial differential equations of the reactive transport model, as mentioned previously.

Section (a, b): a snapshot of CO_2 concentration distribution of the CO_2 concentration versus diameter. the blank regions in section (b) correspond to the positions of the aggregate particles. Similar to the single-phase case, it is observed that CO_2 diffusion is very rapid during the first day of carbonation. However, the presence of aggregates acts as a physical barrier, limiting the CO_2 concentration to less than $5\ Vol\%$ at the center. At 7 days of carbonation, the central CO_2 concentration reaches nearly 8.5 $Vol\%$. After 14 days, a uniform $15\ Vol\%\ CO_2$ concentration is achieved throughout the specimen.

Section (c, d): illustration the impact of aggregates on the CO_2 diffusion, including the aggregates themselves, the CO_2 flux vector field (red arrows), and the diffusion streamlines. The presence of aggregates alters the CO_2 diffusion pattern significantly. This pattern evolves rapidly, eventually approaching a nearly uniform diffusion pattern.

4 Enhancing cement-resistance methodology [63]

Enhancing the performance of cement sheaths for carbon dioxide injection wells can be achieved through two main strategies: either decreasing the permeability of the cement sheath and limiting the quantity of components that interact with CO_2 or introducing a cement type altogether different from conventional Portland cement [40]. Cement varieties that do not fall under the Portland cement category include those based on hydrocarbons-based cement geopolymers (alkali aluminosilicates), calcium sulfoaluminate, magnesium oxide, and calcium aluminate. Studies have shown that calcium aluminate cement exhibits the highest resistance to CO_2 presence because it lacks any constituents that react with carbon dioxide [24][39]. Another approach involves incorporating pozzolanic materials into Portland cement to inhibit corrosion caused by CO_2. The results for this type of modified cement are promising, as it reduces calcium carbonate $CaOH_2$ formation, porosity, permeability, and also enhances compressive strength relative to ordinary Portland cement. Geopolymeric cement systems have demonstrated a significantly lower permeability to CO_2 compared to normal Portland cement formulations.

To achieve an optimal cementing job in the wellbore, several crucial factors must be addressed regarding the cement slurry technology [63]:

- The viscosity of the cement slurry needs to be carefully adjusted so that the dynamic pressure exerted during the cementing operation does not exceed the fracture pressure of the formations.
- The thickening time must be sufficiently long to ensure the safe displacement and placement of the cement slurry along the entire casing length.
- Excessive free water content must be avoided, as well as any sedimentation or particle segregation within the slurry.
- The filtration control properties must be optimized to prevent dehydration or fluid loss from the cement slurry during the cementing process.
- The set cement should develop its designed final compressive strength within the predicted timeframe to enable subsequent completion activities or drilling operations to be carried out as planned.

Meeting these requirements helps ensure the cement slurry can be properly pumped into place and the hardened cement provides zonal isolation with adequate strength and integrity.

4.1 Case study of Žutica and Ivanić oil fields:

Over the years, the Žutica and Ivanić oil fields which were discovered in 1963, have taken place extensive drilling activities, with 303 wells drilled in the Žutica field and 86 wells in the Ivanić field [64][65]. Tertiary phase of EOR from these mature fields were implemented starting in 2001, Specifically, water injection which was initiated into a confined portion of

the reservoir in the Ivanić field, coupled with the suspension of oil production from the same reservoir interval. Subsequently, in 2003, the first cycle of carbon dioxide injection commenced in this reservoir through the well Iva-28 [66]. This marked the beginning of CO_2 enhanced oil recovery operations in the Ivanić field.

Looking ahead, there are further plans to implement the Water Alternating Gas (WAG) enhanced oil recovery method in these fields which involves alternating the injection of water and carbon dioxide to improve oil displacement and sweep efficiency. Additionally, the CO_2 injection operations are scheduled to expand from the Ivanić field to also include the Žutica field, as outlined in the comprehensive Enhanced Oil Recovery (EOR) project for both the Žutica and Ivanić oil fields. According to the plan, by the year 2016, a total of 62 injection wells and 162 production wells will be completed across these two mature fields to facilitate the large-scale EOR operations.

The standard for well design applied to the existing wells on the Žutica oil field consist of:

- Surface casing 339,7 mm ($13\frac{3}{8}$”),
- Intermediate casing 244,5 mm ($9\frac{5}{8}$”)
- Production casing 139,7 mm ($5\frac{1}{2}$")

Whereas the standard well design of the existing wells on Ivanić oil field consist of:

- Intermediate casing 244,5 mm ($9\frac{5}{8}$”)
- Production casing 139,7 mm ($5\frac{1}{2}$") [64][65].

The key requirements for well design specified in the EOR project have to be modified to resist corrosion caused by CO_2:

- The cement used.
- The casing strings (production casing) must withstand an injection pressure of $200\ bar$
- The tubing installed.
- Any packers deployed downhole which exposed to the CO_2 injection fluid.
- All other downhole equipment (subsurface safety valves, gauges, etc.) and surface equipment (wellheads, Christmas trees, flowlines) that will come into contact with the injected CO_2 stream.

Since the existing cement and production casing in the wells are not designed to be corrosion-resistant against CO_2, and pressure testing the production casing to the required 200 bar could lead to severe damage given its deteriorated condition after 50 years of production operations, an alternative approach has been adopted for modifying the injection wells.

The revised design involves lining the existing production casing by installing a new, smaller diameter casing made of corrosion-resistant materials inside it. This inner casing will be designed to withstand carbon dioxide (CO_2) injection and pressure of $200\ bar$, and cemented in place using a cement slurry formulated with CO_2-resistant properties.

The selected sizes for the relining casing are either:

- $101.6\ mm$ (4“)
- or $88.9\ mm$ (3.5”) diameter.

Although relining with new casing offers benefits like corrosion resistance and well stability, there are some drawbacks related to the clearance between the two casings. The clearance between the production casing and relining casing is only $11.35\ mm$ (0.447"):

the $139.7\ mm$ (5 1/2") existing production casing's inner diameter of $124.3\ mm$

and the $101.6\ mm$ (4") relining casing's outer diameter

significantly less than the recommended $19.1\ mm$ (3/4"). This increases dynamic pressure during cementing, risking formation fracturing. Therefore, cementing must be optimized by adjusting the cement slurry's rheological properties and flow rate [12][67]. Figures 4-1 and 4-2 show simulations of annular pressure development during relining casing cementing at Žutica and Ivanić, using optimized cement slurry to reduce dynamic pressure while covering various slurry types. However, slurry optimization alone could not decrease pressure below the formation fracturing pressure, so flow rate optimization was required to match the fracture pressure trend [68][69]

- At Žutica, the flow rate decreased from $400\ dm^3/min$ to $100\ dm^3/min$ before the expected pressure increase with a lower fracturing pressure of $16\ kPa/m$
- At Ivanić, with a lower fracturing pressure of $15\ kPa/m$ the flow rate decreased from $400\ dm^3/min$ to $100\ dm^3/min$, then to $50\ dm^3/min$.

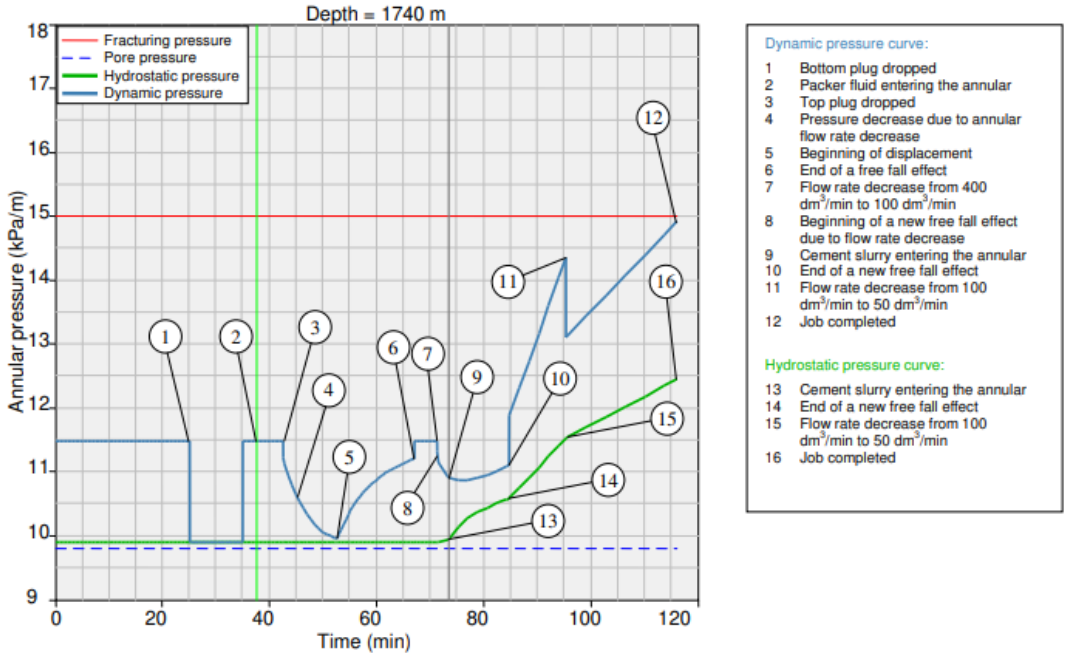

Figure 4-1 Simulation of designing the relining operation on well Iva-70 from [63]

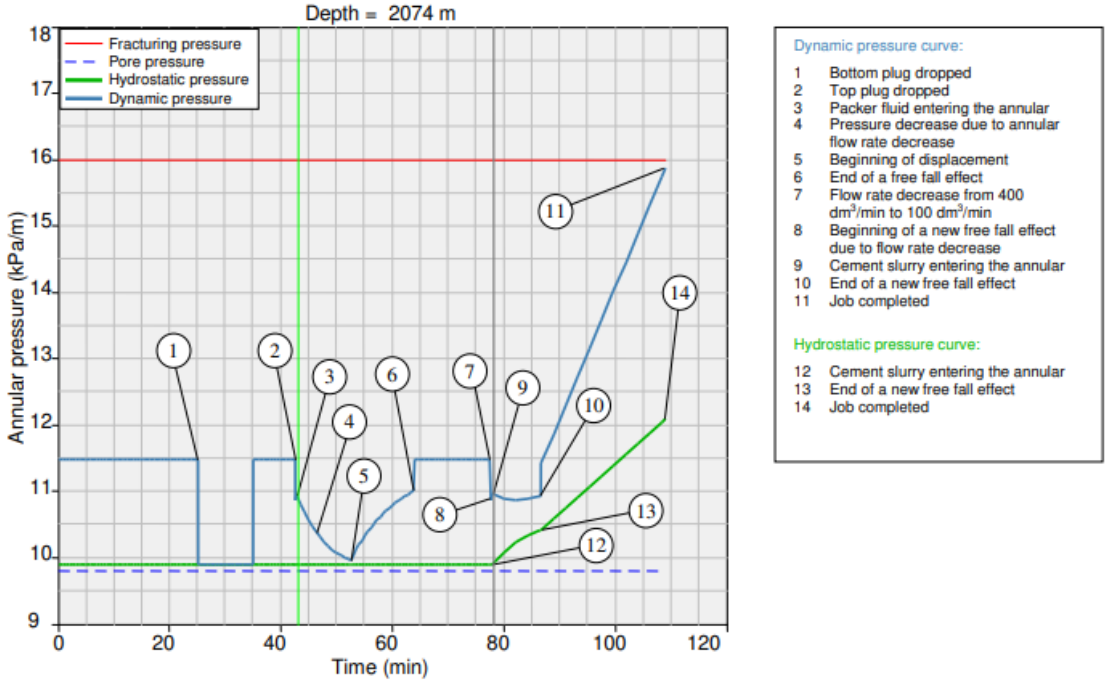

Figure 4-2 Simulation of designing the relining operation on well Zu-111 from [63]

The two operations involved adding a newly formulated cement with less content of $Ca(OH)_2$, with low porosity and permeability to prevent the invasion of carbon dioxide (CO_2) into the formation matrix. Executing these operations had to be optimized to avoid fracturing the formation, while carefully monitoring the flow rate to account for changes during pumping. The clearance between the existing casing and new lining was not

sufficient, so special design and planning were required, as shown in the figures for the two wells. It was also introduced that the casing material had to be corrosion-resistant to carbonation, either by having a high chromium content or by considering the injection of corrosion inhibitors.

In summary, optimizations were made to the cement formulation, flow rates, corrosion resistance of casing materials, and overall operation execution to safely reline the wells while mitigating CO_2 corrosion and formation damage risks.

5 Addition of pozzolanic material

In recent years, many materials and strategies were carried out to resist cement carbonation. One approach involved proposing the use of pozzolanic materials to mitigate carbonation by decreasing the permeability and calcium-to-silicon ratio (C/S) of hydration products [70][71]. Additionally, silica fume and fly ash were also mixed into Portland cement to resist against CO_2 act of corrosion, however, the high silica fume leads cement very difficult to work with because of a high silica fume to cement rate [72][73]. Decreasing the water-to-cement ratio was proposed, but this may increase the risk fractures in cement [73]. Non-Portland cements were suggested to resist CO_2 corrosion although they were not widely applied due to their high cost and lack of proven effectiveness [40]. Some polymer materials additives such as Epoxy resins [74] and latex were used to resist the CO_2 attack [70][72]. While polymer materials just reduce the original permeability of cement matrix, they cannot decrease calcium to silicon ratio (C/S) and CH of hydration products. In Table 5-1, It presents the physical and chemical properties of amorphous calcium aluminate (ACA) including density, viscosity, and main particle size.

Table 5-1 Physical and chemical properties of ACA from [72]

Density g/cm^3	1.56
Viscosity $mPa.s$	150.3
Main particle size nm	$Latex$: 175.2 Sio_2: 56.3 $Pitch$: 206.8
pH	$7.3-7.5$

The thermodynamic principle is employed to carbonation reaction of hydration products. According to this principle, there is a relationship for carbonation reaction at a specific temperature and in CO_2 saturated water which can be written as follow:

$$\Delta G_T = \Delta G_T^0 + RT \ln K$$

Where:

ΔG_T: is Gibbs free energy, KJ/mol

ΔG_T^0 : is Gibbs free energy at same temperature and standard pressure, KJ/mol

R : is a gas constant.

T : is reaction temperature.

K : is reaction entropy.

The ΔG_T^0 of hydration products reaction with CO_2 aqueous solution at different temperature were shown in Table 5-2.

Table 5-2 ΔG_T^0 of reaction between CO_2 aqueous solution and hydration products with different tepretures from [72]

hydration products	ΔG_T^0 25 °C (KJ/mol)	ΔG_T^0 60 °CKJ/ mol)	ΔG_T^0 85 °C (KJ/mol)	ΔG_T^0 127 °C (KJ/mol)
C_3S	−147.75	−128.67	−112.41	−70.78
$C_3S_2H_3$	−72.88	−70.06	−68.23	G0
CH	−38.19	−39.16	−38.76	−39.06
C_2S	−35.14	−29.63	−26.03	−20.26
$C_2SH_{1.17}$	−30.72	−0.19	−12.45	−20.09
$C_5S_6H_{5.5}$	74.32	80.94	89.77	103.76
C_6S_6H	104.59	113.72	137.52	178.39

When Gibbs free energy ΔG_T^0 is low, the reactions are more likely and favorable to occur. Compounds such as $C_3S_2H_3$, C_3S and CH have low Gibbs free energy ΔG_T^0, making them easily attacked by CO_2. Table 5-2 shows that the order of decreasing resistance to carbonation for hydration products at temperature 25 °C to 127 °C:

C_6S_6H, $C_5S_6H_{5.5}$, $C_2SH_{1.7}$, C_2S, CH, $C_3S_2H_3$, C_3S, ettringite (Aft)

Gibbs free energy ΔG_T^0 decreases with the value of C/S increasing.

When cement sufficiently hydrates, compounds like C_2S, C_3S, Aft are present in very small amounts in the hydration products, so they can be ignored. Therefore, reducing the presence of low ΔG hydration products like $C_2SH_{1.7}$, CH and $C_3S_2H_3$ in the cement matrix is an effective measure to enhance the cement's resistance against CO_2 carbonation.

5.1 Carbonation resistant mechanism of ACA

- Decreasing original permeability

Decreasing Original Permeability Reducing the original permeability is an important measure for improving cement's carbonation resistance. When the original permeability is very low, it becomes difficult for CO_2 to invade the cement matrix, thus slowing down the carbonation rate. According to the "grain composition" principle, the addition of ACA introduces non-crystalline SiO_2,, latex, and superfine pitch, which act as good grain compositions with cement particles. These materials fill many macro-pores and micro-fractures in the cement matrix. Additionally, the latex can decrease permeability through "film forming." Therefore, the addition of ACA can decrease the original permeability of the cement matrix and even make it impermeable [72].

- Decreasing CH

The reaction between hydration product CH with CO_2 solution is acid-base reaction and requires low ΔG_T^0, and this is a spontaneous process. CH is consumed by CO_2 and is changed

it into water-soluble $Ca(HCO_3)_2$, which diffuses out of cement matrix increasing porosity and permeability, while decreasing compressive strength. Non-crystalline SiO_2 can decrease the CH by converting it into carbonation resistant products cementing $C-S-H$. The process can be expressed the following reaction When CH is changed into $C-S-H$, the leaching effect is weakened [72]

$$Ca(OH)_2 + SiO_2 \rightarrow C-S-H$$

The content of CH is an important indicator to carbonation resistance capability of cement. A lower CH suggests improved carbonation resistance as CH was consumed by non-crystalline SiO_2 and generated erosion-resistant cementing products, such as $C_5S_6H_{5.5}$ and C_6S_6H. Meanwhile, the acid-base reaction is weakened due to the consumption of CH [72].

- Decreasing C/S and increasing ΔG_T^0

The addition of ACA decreases C/S ratio and increases the activation energy ΔG_T^0 of the products making carbonation reaction more difficult. low C/S hydration products $C-S-H$ are formed due to non-crystalline SiO_2 reaction with the products $C-S-H$ (high C/S). A decrease in the C/S of products means that the activation energy ΔG_T^0 of cement hydration products is increased requiring more energy during carbonation process.

The C/S of the products $C_5S_6H_{5.5}$ and C_6S_6H is much lower than $C_3S_2H_3$, making the carbonation reaction more difficult. The decrease in products $C-S-H$ (high C/S) can also weaken dissolution effect, which makes $C-S-H$ change into amorphous silica gel (SiO_xOH_x) [72].

5.2 The effect of adding ACA material

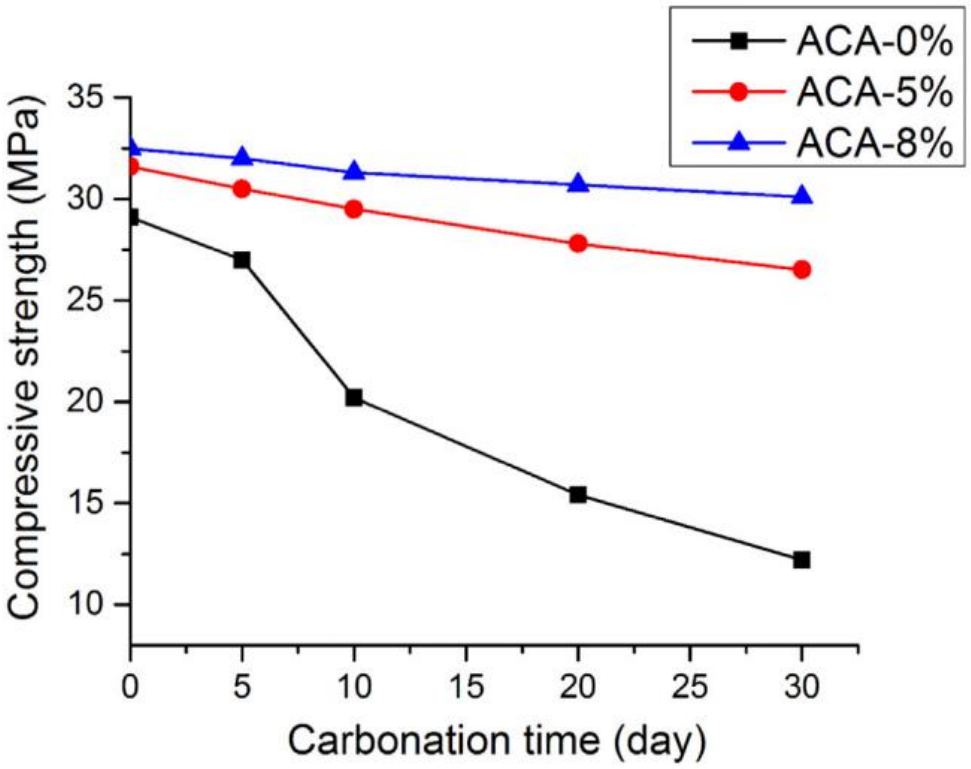

Figure 5-1 The compressive strength of samples with different content of ACA from [72]

The figure 5-1 shows that initial compressive strength of samples, which were added ACA, is higher compared to sample $ACA - 0\%$ (without ACA). This is because the ACA 's latex and superfine pitch particles fill the macro-pores and micro-fractures in the cement matrix. Additionally, these latex and pitch particles can absorb fracture energy, thereby preventing crack initiation and propagation [72][75].

The figure also clearly demonstrates that the compressive strength of all cement samples decreased over carbonation time. However, the compressive strength of sample ACA -0% decreased very rapidly, whereas the compressive strength decreased slowly with the addition of ACA increasing.

For instance, after 30 days of exposure to the carbonation brine, the compressive strength of the $ACA - 0\%, ACA - 5\%, and\ ACA - 8\%$ samples decreased by $58.08\%, 16.14\%$ and 7.38%, respectively compared to their initial values.

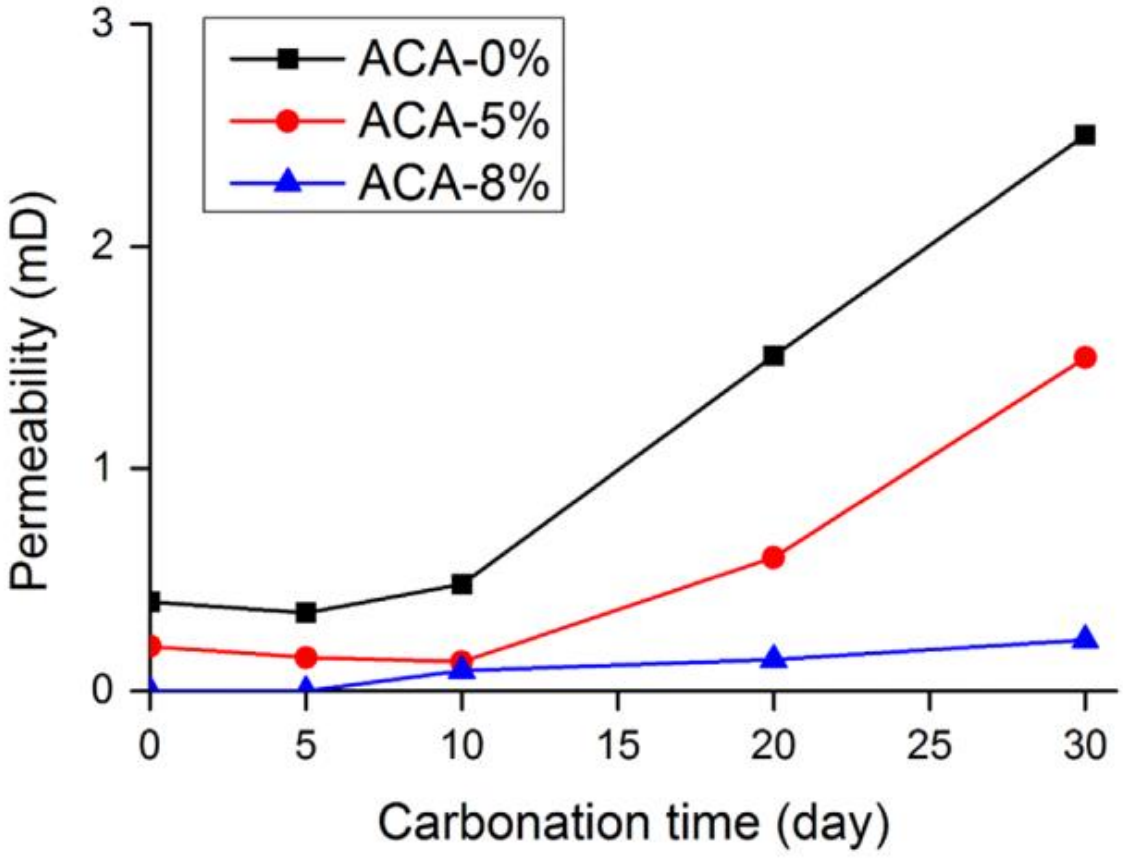

Figure 5-2 the permeability of cement samples with different content of ACA from [72]

The permeability of cement samples was measured according to Darcy's law, and the results are shown in Figure 5-2. This figure indicates that the permeability of samples initially decreased in the first 10 days and then increased over the latter 20 days.

The initial permeability reduction may be attributed to some pores being filled by carbonation products and a weak leaching effect. The subsequent increase in permeability could be due to the leaching effect and dissolution, leading to the consumption of CH, which changes into soluble $Ca(HCO_3)_2$, and the conversion of $C-S-H$ into amorphous silica gel.

For ACA -0% sample, the permeability changed from $0.4\ mD\ to\ 2.5\ mD$ when it was in carbonation brine for 30 days.

However, for the ACA -8% sample, the permeability only slightly increased under the same conditions.

There are two reasons for the improved permeability performance of the samples after the addition of ACA:

- First, the non-crystalline SiO_2, latex, and superfine pitch particles fill some macro-pores and micro-fractures, decreasing the original permeability of the samples.

- Secondly, the film-forming effect of latex can prevent gas invasion.

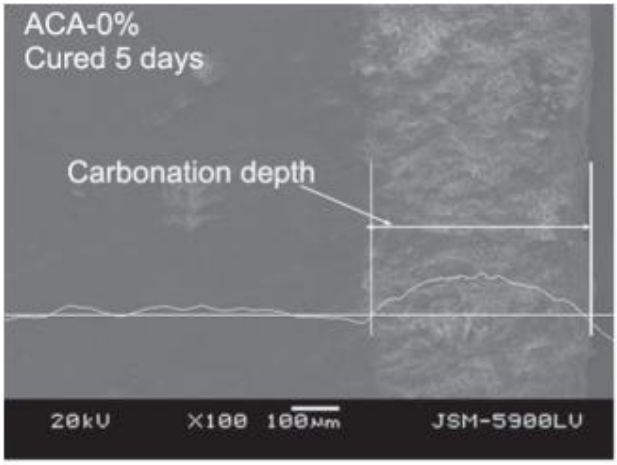

(a) ACA-0% cement sample carbonation depth

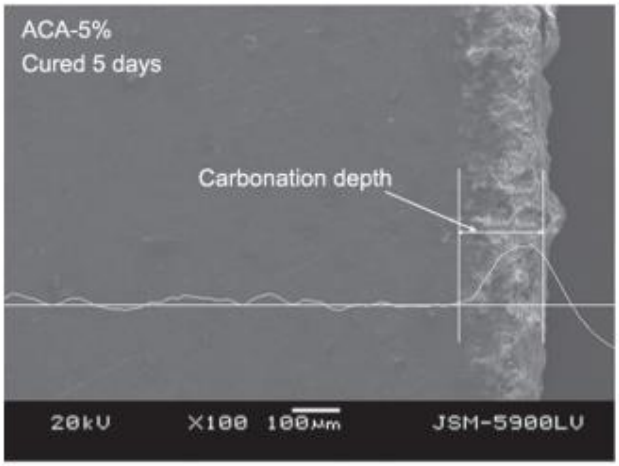

(b) ACA-5% cement sample carbonation depth

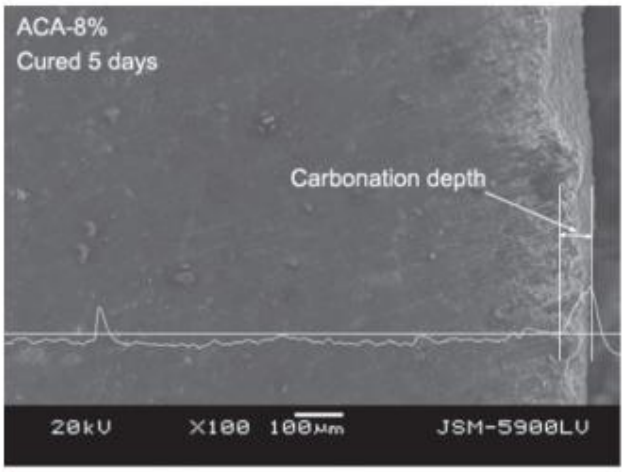

(c) ACA-8% cement sample carbonation depth

Figure 5-3 Carbonation depth with different content of ACA from [72]

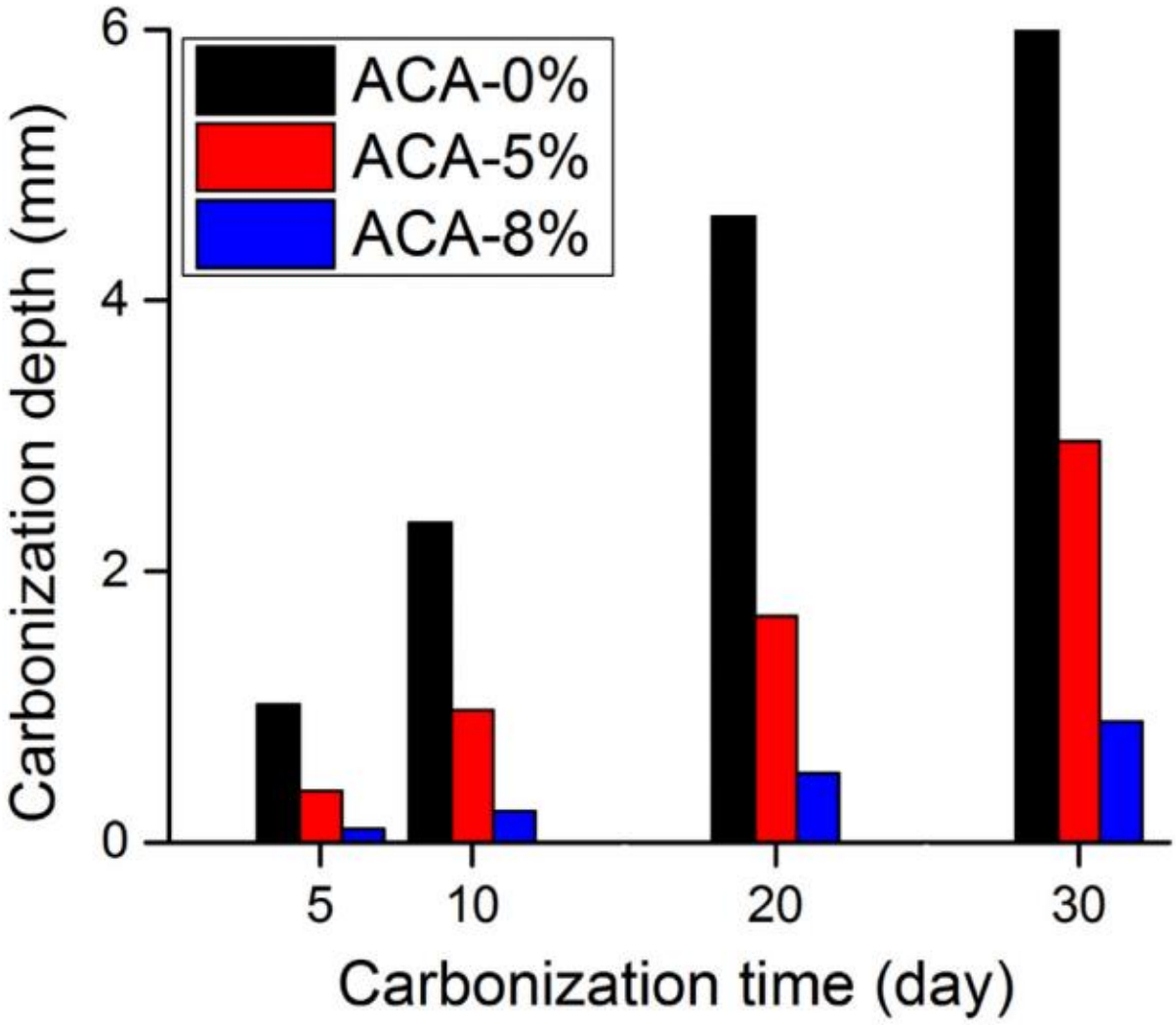

Figure 5-4 carbonation depth with respect to time from [72]

Figures 5-3 and 5-4 demonstrate that the carbonation depth decreased with increasing ACA addition and increased with longer exposure time. After the cement samples were carbonated for 10 days, a clear carbonation interface was observable in the figure 5-3.

The ACA-0% sample exhibited substantial carbonation, whereas the ACA-8% sample showed only light carbonation.

Comparing the carbonation depth of samples with different ACA concertation after 30 days of exposure to the carbonation brine, it is evident that the carbonation depth of the ACA -0% sample was $6.11\ mm$, while that of the ACA -8% sample was only $0.89\ mm$

As the carbonation time increased from $5\ days\ to\ 30\ days$, the carbonation depth of the samples increased as follows:

$$ACA\ 0\% -\ 5.09\ mm,$$

$$ACA\ 5\% -\ 2.58\ mm$$

$and\ ACA\ 8\% -\ 0.88\ mm$

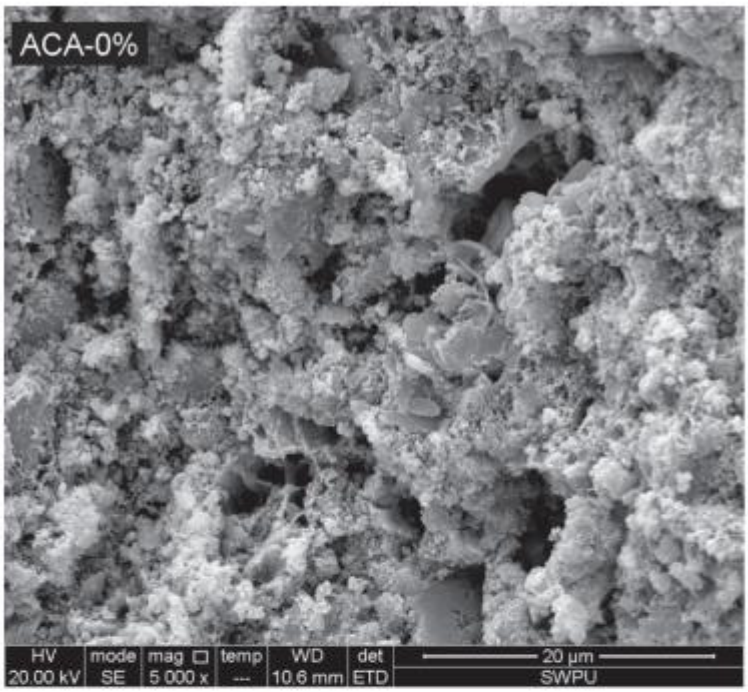

(a) ACA-0% cement sample

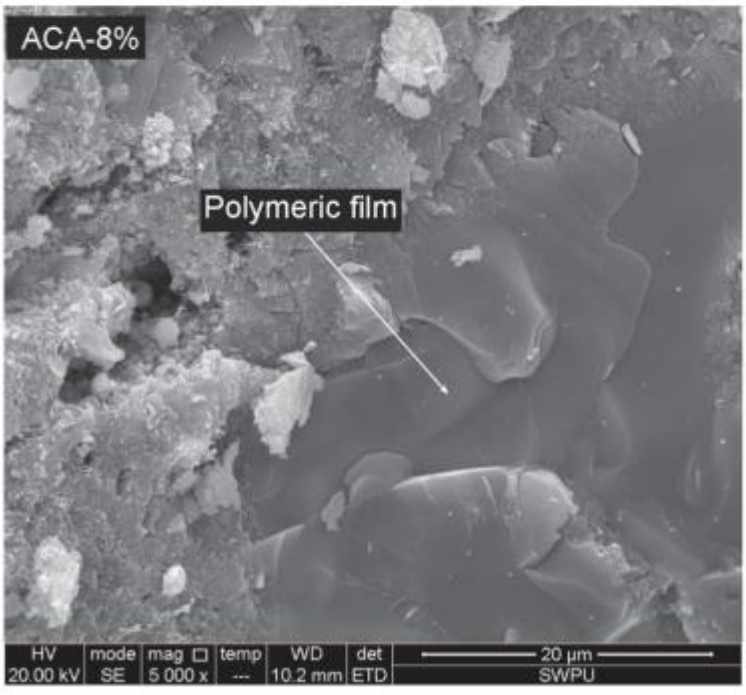

(b) ACA-8% cement sample

Figure 5-5 The scanning electron microscopy (SEM) images of cement sample with different content of ACA from [72]

Figure 5-5 shows the scanning electron microscopy (SEM) images of the carbonation interfaces for the ACA -0% and ACA -8% cement samples. It reveals that the interface of

the ACA -0% sample is very loose (a) and contains numerous pores. This porous structure is attributed to the corrosion product $CaCO_3$ being converted into soluble $Ca(HCO_3)_2$, which then diffuses out of the cement matrix [76][72]. Additionally, the presence of original cementitious pores, capillary pores, transition pores, and micro-fractures contribute to the porosity [77][72].

In contrast to the ACA -0% sample, the ACA-8% sample exhibits a few pores and a compact interface, with a distinct polymeric film observed on the carbonation surface (b). This observation suggests that polymeric film can prevent the invasion of the carbonation brine [72].

6 Addition of Basalt powder

Basalt powder has gained attention as a potential supplementary cementitious material in cement paste (SCM) and composites (SCM reinforced polymers) [79][78] offering an alternative to enhance the chemical resistance of cement. However, further studies are required to evaluate the performance of these materials in representative conditions of carbon capture and storage (CCS) storage sites. Even minute amounts of SCMs can alter the quantity and nature of hydration products formed within the cement matrix, refining the porous structure, which could delay carbonation and improve wellbore integrity [80]. Furthermore, there is no consensus solution on the use of SCM (conventional or unconventional) in cement formulations to mitigate the effect of acid gases [81]. Thus, Numerous aspects concerning the type and quantity of SCMs required to tailor the properties of cement pastes for applications in CO2-rich environments need to be addressed. Therefore, an adequate understanding of the cement carbonation process can allow to obtain properties of the new formulations to be adjusted to the requirements of the future CCS projects [82]

In this context, basalt powder (BP), a natural SCM, could be added to cement formulations to enhance the material's resistance against prolonged exposure to CO_2. [82][78]. Basalt, an igneous rock, exhibits low pozzolanic activity and can be employed as an SCM, either as a partial replacement for cement powder or as an additive to cement pastes in novel formulations [83].

Basalt powder is a by-product of mining process and its use in cement paste for wells can offer environmental and financial benefits, as the raw material cost is lower, and a portion of the CO_2 emissions from clinker production is avoided [84]. Basalt powder is readily available and possesses characteristics that recommend its use as an SCM, making it a potential candidate for commercial-scale applications.

Previously, the chemical resistance of cement pastes formulations with the addition of $0\%, 6\%, 9\%$ and 13% basalt was evaluated [85]. Despite obtaining positive results, the study based its conclusions on merely four cement specimens (one per formulation), which underwent a degradation process in brine solution under mild experimental conditions (65°C and 75.8 bar CO2). Furthermore, a comprehensive characterization of the cement formulations after exposure to CO2 was not performed due to the compromised state of some specimens following the degradation test. Consequently, it is proposed a study on the use of BP as an SCM in well cement formulations to enhance the material's performance in a supercritical CO2 environment. The BP was added in varying concentrations to API class G cement, and cement paste carbonation was carried out simulating CCS reservoir conditions. The new formulations were investigated to evaluate the effect of BP addition on the properties of the cement paste, define the ideal mixture composition, and identify the formulation exhibiting the best chemical and mechanical performance. The evaluation of the chemical and mechanical performance of the new materials when exposed to supercritical CO2 was conducted through comprehensive experimental characterization. Thus, by

incorporating a natural SCM, the aim is to propose a cement formulation capable of increasing wellbore integrity in CCS operations and present a low-cost solution to improve cement paste stability in CO2-rich environments.

6.1 Materials and Methods

The study evaluates the integrity of cement paste formulations prepared by mixing API class G cement and BP as an SCM. The new formulations, containing BP in concentrations ranging from 0.25% to 5% by weight, were subjected to wet carbonation under supercritical CO2 conditions, simulating the CCS storage environment. The formulations were evaluated using a series of analytical methods before and after undergoing the CO2 degradation process.

The chemicals used in this formulation are:

- calcium oxide (95%),
- hydrochloric acid (37%),
- saccharose (analytical grade)
- and phenolphthalein (analytical grade)

which were used without further purification. The composition of the cement used are provided below in table 6-1:

Table 6-1 Chemical composition of class G cement from [78]

Chemical composition	Percentage [%]
SiO_2	29.25
Al_2O_3	3.95
Fe_2O_3	4.57
CaO	65.07
MgO	2.32
SO_3	2.27
Na_2O	0.25
K_2O	0.33
Class G Characterization	**Surface area [$m^2 \cdot g^{-1}$]**
BET specific surface area	0.77
Langmuir specific surface area	2.69
[a]Average particle size (Å)	78,103.0

Basalt was obtained from local suppliers as a coarse aggregate for civil construction purposes. The basalt powder (BP) was produced through ball milling and material sieving processes. the powder was manually sieved through mesh and utilized as the supplementary cementitious material (SCM) [78].

6.2 Experimental results from Gabriela research [78]:

The basalt powder exhibited varied particle sizes with irregular shapes, rough surfaces, and diverse granulometry. While the larger particles displayed undefined rounded edges, potentially related to the abrasion fragmentation mechanism during ball milling [81], the smaller particles exhibited irregular shapes, rough surfaces, and sharper edges, likely associated with the different cleavage planes due to the diverse mineralogical composition of basalt [83]. Comparing the BET specific surface area of basalt powder $(5.41\ m^2/g)$ with class G cement $(0.77\ m^2/g)$ revealed that BP has a higher specific surface area and smaller particle size. Thus, the morphological and surface characteristics of BP particles are expected to be relevant to the mechanical and rheological properties of the cement paste [78][81]. The irregular shapes of the smaller particles contribute to a high relative specific surface area, decreasing cement paste hydration and reducing the cured material's pore size and permeability [46]. Conversely, the slightly rounded edges of the larger particles improve the cement paste flowability and reduce stress concentration, making the specimens less prone to cracking [81][78]. Furthermore, particles with sharper edges typically create more resistance to mixture rheology and increase the water demand for cement hydration due to the increased specific surface area [81][78]. The small BP content added to the proposed cement formulation resulted in only a slight difference from the cement without BP addition.

After identifying the morphological and surface characteristics of the basalt powder, the mineral composition of the raw material was characterized using X-ray diffraction (XRD) (Table 6-2). The mineral composition of the SCM defines its reactivity during the hydration process, the role it plays in the cement formulation, and indicates the mineral phases generated after curing [78].

Table 6-2 Mineral composition of basalt powder from [78]

XRD Mineral Composition	Abbreviation	Value
Quartz [wt.%]	Q	9.9
Andesine [wt.%]	A	37.8
Sanidine [wt.%]	S	5.4
Augite [wt.%]	Px	27.9
Forsterite iron [wt.%]	F	1.6
Ilmenite [wt.%]	I	2.5
Goethite [wt.%]	G	0.3
Orthoclase [wt.%]	O	11.4
Magnetite [wt.%]	M	3.1
Basalt Powder Characterization	**Abbreviation**	**Value**
BET specific surface area [$m^2 \cdot g^{-1}$]	BET	5.41
Langmuir specific surface area [$m^2 \cdot g^{-1}$]	LSA	51.22
Pozzolanic Activity Index [mg $Ca(OH)_2$]	$I_{Ca(OH)2}$	180.2
[a] Average particle size (Å)	APS	11,097.3

Table 6-2 shows that BP is primarily composed of:

- $Andesine$ (37.8%),
- $Augite$ (27.9%),
- $Orthoclase$ (11.4%),
- $and\ Quartz$ (9.9%),

with minor mineral phases including:

- $Sanidine$ (5.4%),
- $Magnetite$ (3.1%),
- $Ilmenite$ (2.5%),
- $Forsterite\ iron$ (1.6%),
- $and\ Goethite$ (0.3%).

These minerals have been previously reported in basalt powders applied as $SCMs$ in cement and concrete formulations, indicating that BP may exhibit slightly pozzolanic activity during the hydration process, consuming cement portlandite and increasing the production of calcium-silicate-hydrate $(C-S-H)$ phases [83][78], and/or presenting a filler effect due to the smaller particle size, reducing porosity by occupying empty spaces in the cured material [78][52]. To complement the morphological, mineralogical, and surface area analyses, the pozzolanic activity of the basalt powder was evaluated using Chapelle's method (Table 6-2). Chapelle's analysis assesses the pozzolanic activity of SCMs based on the indirect measurement of portlandite consumption during the hydration process, enabling verification of the role BP will play in the cement paste formulation. A higher portlandite consumption leads to greater formation of secondary mineral phases in the cementitious matrix [46][78], influencing the chemical and physical properties of the cement paste by reducing porosity, increasing compressive strength, and reducing chemical degradation by CO_2. Based on the pozzolanic activity results, BP consumed $180.2\ mg$ of $Ca(OH)_2$ during the Chapelle test, which is less than the $330\ mg\ Ca(OH)_2$threshold defined by Raverdy [86] for an SCM to be considered a highly active pozzolanic material. Although BP contains a substantial amount of silica- and alumina-rich minerals, its low pozzolanic activity has been previously identified and is explained by the lack of vitreous phases and the presence of highly crystallized minerals [78]. Thus, based on the characterization results (Table 6-2), basalt powder can be used as a filled-pozzolanic material, being partially consumed in the cement hydration process, and occupying the porous spaces of the material.

It is known that curing conditions (temperature and pressure) can influence the properties of the cement sheath. To prevent strength retrogression in wells operating at temperatures above $110°C, 35-40\%$ crystalline silica is typically added relative to the weight of cement $(BWOC)$ [78][82]. Unlike highly pozzolanic crystalline silica, BP exhibits low reactivity and a large inert mineral fraction. Therefore, due to the low pozzolanic activity of basalt powder, it is unlikely that BP can replace crystalline silica as an additive in high-temperature cement formulations. Future work should evaluate the feasibility of using mixtures of crystalline

silica and basalt powder in high-temperature CCS wellbore cements, as well as studying the effect of CO2 on the chemical and mechanical resistance of these formulations.

After characterizing the basalt powder and preparing the cement formulations, CO_2 degradation tests were performed to evaluate the chemical resistance of the cement specimens. Figure 6-1 shows images obtained from the $BP\ 0.00$ (neat cement paste) and $BP\ 0.25$ (cement paste containing $0.25\ wt.\%\ BP$) samples after exposure to CO_2-saturated water at $15\ MPa$ and $65°C\ for\ 7$ days, illustrating the chemically altered layer depth highlighted using phenolphthalein solution. The carbonation results exhibited typical CO_2 degradation behavior in the cement matrix, as evidenced by the reduction of the pink area (indicating the presence of portlandite) and an increase in the carbonated grey area, highlighting the degraded fraction of the material [78][86]. The pink color in the central portion of the cement specimens is associated with the interaction of phenolphthalein solution with the alkaline reserve of the cement paste, mainly due to the preservation of the portlandite (CH) fraction, indicating an absence of the CO_2 degradation process. In contrast, the grey portion at the edges of the cement specimens demonstrates a high consumption of CH, indicating pH neutralization and the formation of calcium carbonates ($CaCO_3$) [78].

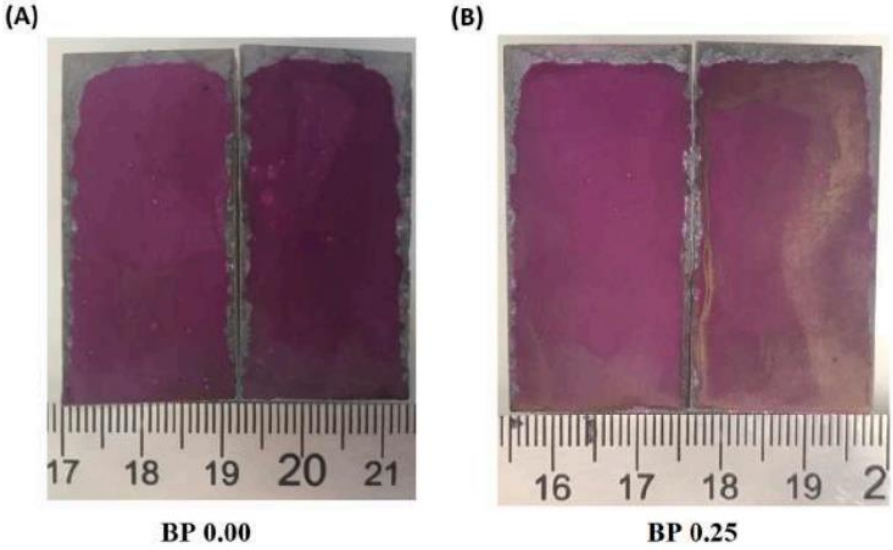

Figure 6-1 samples after exposure to CO_2-saturated water at $15\ MPa$ and $65°C$ for 7 days from [78]

The reference cement paste ($BP\ 0.00$) shows an extended degraded layer in comparison with $BP\ 0.25$. These results suggest that the addition of the mineral filler improved the cement's chemical performance when exposed to the corrosive medium with supercritical CO_2. Moreover, it can be assumed that the addition of basalt powder reduced the sample's permeability, making the cement paste more resistant to CO_2 intrusion. The chemical resistance of the cement formulations was evaluated by measuring the carbonated layer (CL) and carbonated volume (CV) of the specimens, with the results shown in Table 6-3. Since the degradation fronts do not advance homogeneously along the specimen, the CV was also estimated to obtain a more accurate measurement of the degraded fraction of the cement specimens.

Table 6-3 Various samples exposure to CO_2-saturated water at 15 MPa and 65°C for 7 days [78]

Sample	BP [wt.%]	W/S	CL[a] [mm]	CV[b] [mm³ %]
BP 0.00	0.00	0.440	1.25 ± 0.58	20.40
BP 0.25	0.25	0.439	0.86 ± 0.11	15.91
BP 0.50	0.50	0.438	1.17 ± 0.17	19.73
BP 1.00	1.00	0.436	1.21 ± 0.23	20.65
BP 2.50	2.50	0.429	1.21 ± 0.18	32.83
BP 5.00	5.00	0.419	1.06 ± 0.05	30.15

BP - Basalt Powder; W/S – Water-to-Solids Ratio; CL - Carbonated Layer; CV - Carbonated Volume.

Table 3 shows that, with the addition of BP to the cement, there is an initial reduction of the carbonated layer in relation to the reference (BP 0.00), and the best result was obtained for the formulation containing $0.25\ wt.\%$ of basalt powder (BP 0.25). Then, the extent of the carbonated volume increases from BP 0.50 to BP 5.00, demonstrating that small additions of SCM can increase the material's resistance against CO_2 chemical degradation, while higher basalt powder contents reduce the chemical resistance of the cement formulations. Furthermore, cement formulations with higher water-to-solids ratios, BP 0.25 ($W/S = 0.439$) and BP 0.50 ($W/S = 0.438$), have greater resistance to carbonation than samples with higher density:

BP 1.00 ($W/S = 0.436$) ,

BP 2.50 ($W/S = 0.429$),

and BP 5.00 ($W/S = 0.419$).

From these results, it was found that cement formulations with low basalt powder content ($\leq 0.50\ wt.\%$) exhibit the best chemical resistance to CO_2, confirming the literature statement that even small SCM additions can significantly alter the properties of the cement paste [78][67]. However, the literature argues that cement formulations with higher density are expected to have greater resistance to carbonation, this change may be related to the basalt powder characteristics.

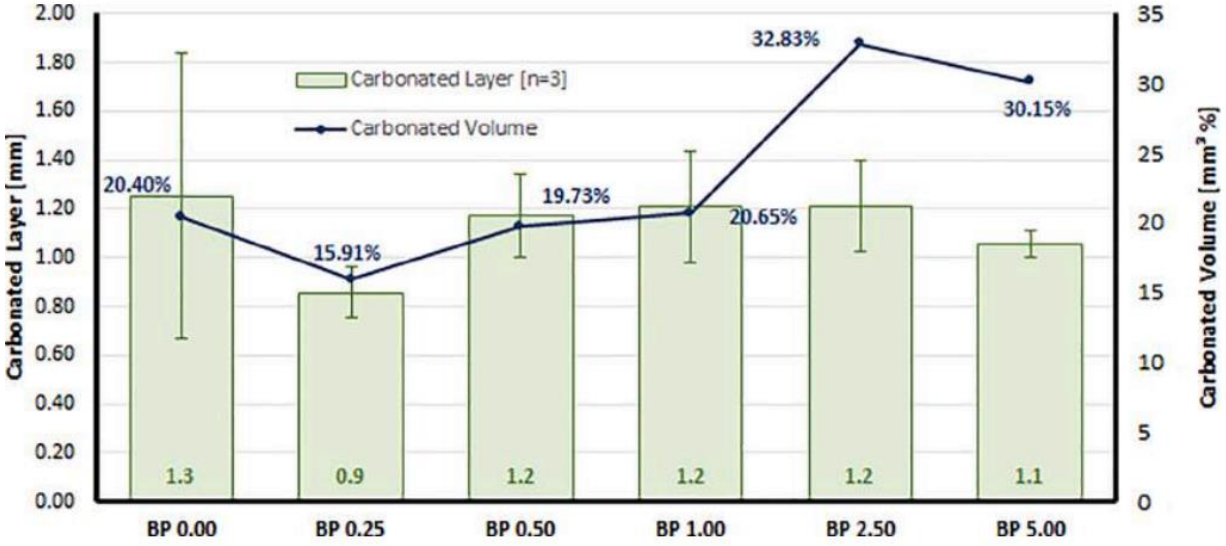

Figure 6-2 The extent of carbonation with different BP concentrations from [78]

Figure 6-2 shows that the extent of carbonation estimated by both the phenolphthalein method and Micro-CT analysis present a reasonable agreement. The micro-tomography results corroborate the phenolphthalein test profiles, in which the cement pastes with low contents of BP ($\leq 0.50\ wt.\%$) present better performance. The formulations $BP\ 0.25$ and $BP\ 0.50$ show superior results in terms of resistance against CO_2 degradation when compared to formulations with neat cement paste ($BP\ 0.00$) and those formulations with higher BP contents ($BP\ 1.0, BP\ 2.50, and\ BP\ 5.00$). Such improvement in the properties of porosity, permeability, and chemical resistance to CO_2 is attributed to small additions of BP, since the cement formulations with higher water-to-solids ratios, $BP\ 0.25$ ($W/S\ =\ 0.439$) and $BP\ 0.50$ ($W/S\ =\ 0.438$), have greater resistance to carbonation than samples with higher density:

$BP\ 1.00$ ($W/S\ =\ 0.436$),

$BP\ 2.50$ ($W/S\ =\ 0.429$),

and $BP\ 5.00$ ($W/S\ =\ 0.419$).

The micro-CT results reinforce the conclusion that the addition of basalt powder at low contents increases the cement paste's resistance to the CO_2-rich medium by refining the porous structure and reducing the cement sheath permeability. Thus, to confirm these statements, the porosities of the initial (non-carbonated) and final (carbonated) cement specimens were estimated from the micro-CT data processing, and the results are presented in Table 6-4.

Table 6-4 Porosity profile before and after carbonation [78]

Sample	BP [wt.%]	W/S	IP [mm^3 %]	FP [mm^3 %]
BP 0.00	0.00	0.440	0.49	0.40
BP 0.25	0.25	0.439	0.12	0.08
BP 0.50	0.50	0.438	0.08	0.08
BP 1.00	1.00	0.436	0.66	0.60
BP 2.50	2.50	0.429	1.06	1.28
BP 5.00	5.00	0.419	0.35	0.29

BP - Basalt Powder; W/S – Water-to-Solids Ratio; IP - Initial Porosity; FP - Final Porosity.

The influence of basalt powder addition on the mechanical strength of the cement formulations was evaluated both before and after the carbonation process. Compressive strength after carbonation is an important property to be measured since calcium carbonate precipitation can positively influence the cement paste porosity at the beginning of the degradation process [87]. The compressive strength results are detailed in Table 6-5. The non-carbonated samples' compressive strengths ranged from $23.7\ to\ 57.7\ MPa$, while the carbonated samples' compressive strengths ranged from $33.7\ to\ 52.7\ MPa$. It is well known that porosity can influence both microscopic properties (in this case, CO_2 diffusivity) and macroscopic properties, such as the compressive strength of a cementitious material.

Table 6-5 compressive strength profile before and after carbonation [78]

Sample	BP [wt.%]	W/S	IC [MPa]	FC [MPa]
BP 0.00	0.00	0.440	28.0 ± 3.6	42.0 ± 8.9
BP 0.25	0.25	0.439	23.7 ± 3.1	45.3 ± 7.5
BP 0.50	0.50	0.438	57.7 ± 4.2	52.7 ± 18.8
BP 1.00	1.00	0.436	50.7 ± 13.6	40.0 ± 4.0
BP 2.50	2.50	0.429	42.3 ± 5.0	42.7 ± 2.4
BP 5.00	5.00	0.419	45.7 ± 10.2	33.7 ± 11.4

BP - Basalt Powder; W/S – Water-to-Solids Ratio; IC - Initial Compression; FC - Final Compression.

From table 6-5, it is possible to observe a positive effect of basalt powder on the initial compressive strength of cement specimens with high BP contents ($\geq 0.50\ wt.\%$), despite the increase in porosity. For both non-carbonated and carbonated samples, there is an initial increase in compressive strength, with the maximum being obtained for the sample with $0.50\ wt.\%$ of basalt powder ($BP\ 0.50$). This is followed by a reversal in the trend for the cement specimens with high BP contents and low water-to-solids ratios

$BP\ 1.00 - W/S = 0.436;$

$BP\ 2.50 - W/S = 0.429;$

$BP\ 5.00\ -\ W/S\ =\ 0.419.$

Regarding the influence of carbonation on the cement's mechanical properties, only for samples with low basalt powder content and high water-to-solids ratios ($BP\ 0.25\ -\ W/S\ =\ 0.439$; $BP\ 0.50\ -\ W/S\ =\ 0.438$) was the final compressive strength (carbonated samples) higher than that initially measured (non-carbonated samples). Otherwise, the loss in mechanical strength is clearly seen for samples with high contents of basalt powder ($BP\ 1.00, BP\ 2.50, and\ BP\ 5.00$), since the final compressive strength is lower than that measured before the carbonation process.

As previously discussed, the low pozzolanic reactivity and the high inert fraction of the basalt powder can lead to a delay in the hydration process, resulting in an unreacted BP fraction, changing the spacing of the cement matrix and resulting in an increased porosity and permeability of the cement formulations with high BP contents ($BP\ 1.00$, $BP\ 2.50$ and $BP\ 5.00$). These modifications in the cement structure increase degradation by CO2 and reduce the mechanical properties of the cement after carbonation. Furthermore, these characteristics may be influenced by the low availability of water in formulations with high basalt powder content:

$BP\ 1.00\ -\ W/S\ =\ 0.436$;

$BP\ 2.50\ -\ W/S\ =\ 0.429$;

$BP\ 5.00\ -\ W/S\ =\ 0.419$).

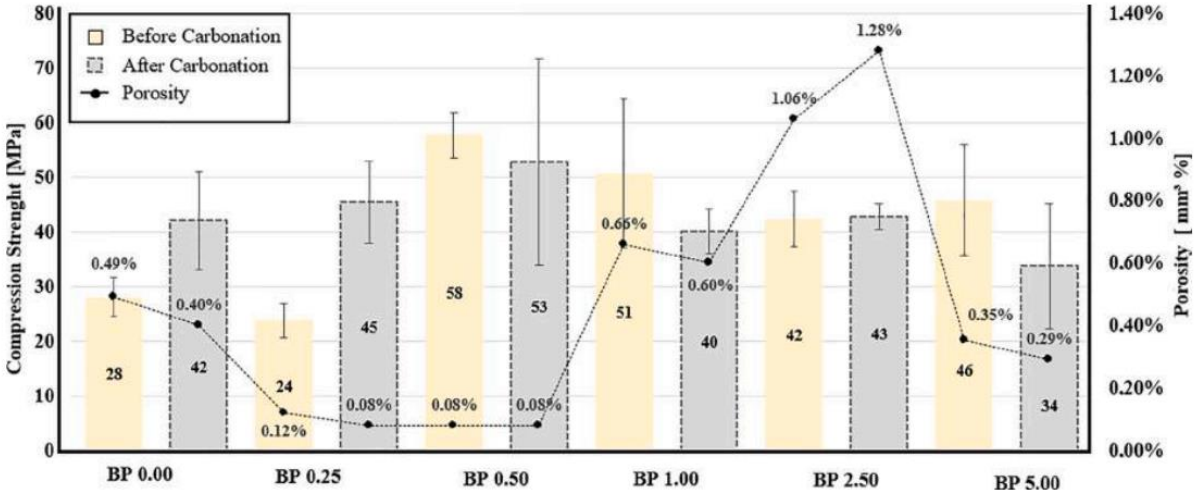

Figure 6-3 Both porosity and compressive strength of cement with basalt powder before and after carbonation from [78]

Shown in the figure 6-3 $BP\ 0.50$ has the highest compressive strength, which is slightly compromised by the carbonation process, and the lowest porosity value, which is practically unchanged by the degradation process. Thus, it can be concluded that low basalt content in the cement paste can modify the cement's microstructural properties, such as porosity, for example. However, these changes are not enough to promote significant differences in the

material's macrostructural properties, such as compressive strength. Otherwise, the $BP\ 1.00, BP\ 2.50$ and $BP\ 5.00$ cement formulations have a significant loss of compressive strength after the carbonation process (less pronounced for $BP\ 2.50$), while having porosity values substantially higher than the reference sample ($BP\ 0.00$). Although calcium carbonate can fill the pores and reduce the cement porosity, the larger pores cannot be filled. Thus, the porosity can be reduced with no significant changes in the mechanical strength.

7 The use of Nanoparticles in cement.

This investigation concentrates on innovative solutions to enhance the properties of cement, with a significant attention on the capabilities of nanotechnology to improve the characteristics of cement. Generally, the focus is on the G class cement for the next nano-technology approach. The application of nanotechnology with cement can improve:

- cement elasticity,
- strength,
- self-cleaning,
- and electrical conductivity [88].

There are several contributions through nanotechnology application in cementing:

- Santra et al. demonstrated the effects of nanomaterials on early cement slurry gelation, compressive strength ratio, viscosity enhancement, and early-stage compressive strength [102].
- Ershadi et al. pointed out that nanomaterials have reduced cement slurry thickening time [102].
- Fakoya and Shah discussed the application of nanosilica in the oil industry and cementing operations. It was illustrated that nanosilica could reduce drag in porous media, has been effective in water invasion in shale, and has been applicable in fluids rheology control [88].
- Thakkar et al. have demonstrated the application of nanosilica as an alternative to conventional cement additives like calcium chloride and silica. From this perspective, the consumption of nanosilica was much smaller than the others, and it has been multi-functional. Due to the use of nanosilica, decreases in thickening time, increases in compressive strength, and decreases in fluid loss have been reported. Moreover, they have reported (2019) a decrease in the Wait on Cement (WOC) time and, therefore, a reduction in the overall capital cost of a well due to the use of nanosilica [89][100].

A nanofluid is a fluid species in which nanoparticles are dissolved in an approximate diameter of 10 nm in liquid. The presence of these particles causes the cement pattern to change completely, and the way the molecules and layers are located. Therefore, in the case of correct selection of this material, very favorable conditions can be obtained at a very low cost compared to other methods [99].

The use of nano particles into the cement slurry can decrease the permeability to CO_2 injected and therefore as the previous approaches it can increase the resistivity to corrosion act of CO_2 and provide the well with more lifetime and more stability. Furthermore, the effect of nano particles was not tested in injection environment, but it has a promising future through the industry. Through the investigation, it is provided the tests and

permeability reduction of cement slurry in laboratories experiments conducted by Mahmoud Bayanak et al [88]

7.1 Material and method

The composition of cement slurry used in this study:

- Nanosilica (SiO2 with 99% purity and $50-60\ nm$ in diameter) made by "Nanoshell" Company (USA),
- G-class cement (API standards)
- water,
- dispersants,
- fluid loss controls,
- retarders,
- gas migration additive,
- antifoam,
- and extender were employed.

Most cement additives have trade names. For example, extender $D-124$ is a material composed of hollow spheres of aluminosilicate with a specific gravity lower than water. The particle size, like silica flour, enables blending the material with cement to form a slurry with density as low as $9.0\ PPG$.

Through the experiment it was used two main slurries with densities of $90\ PCF$ and $120\ PCF$.

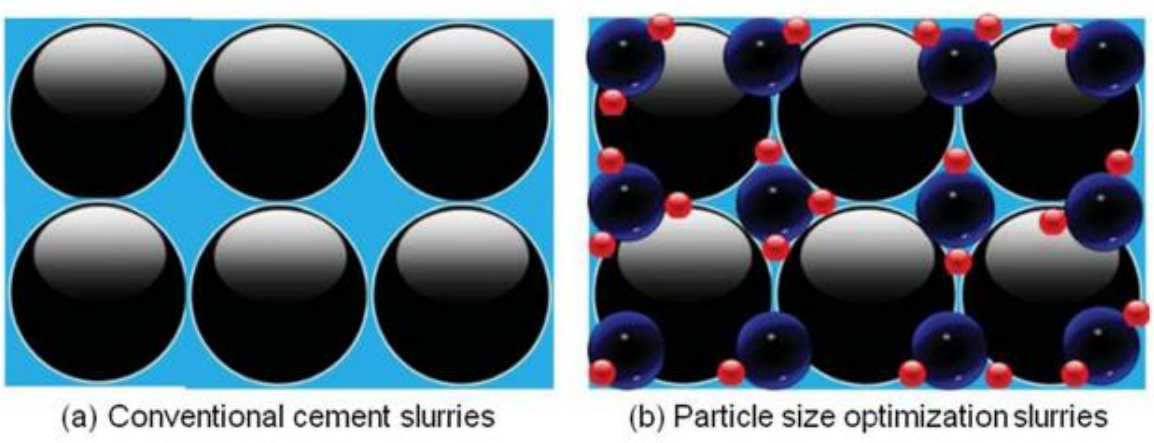

Figure 7-1 Cement matrix compressibility [88]

7.2 FMA analysis

The FMA realistically simulates wellbore parameters like:

- temperature,
- hydrostatic head pressure,
- formation fluid pressure,
- and pressure gradients driving invasive fluid flows.

The FMA test cell resembles an API HTHP fluid loss cell. A hollow hydraulic piston at the top applies pressure to simulate hydrostatic effects on the cement. Filtrate from the slurry can be collected from screens/cores at the top and bottom.

For the first condition Figure 7-2 showed the gas migration analysis results. The test duration was 4-5 hours with around 6 mL of gas migration based on the chart.

Figure 7-2 Gas migration results (green) for 95 PCF with 0.3% nanoparticles [88]

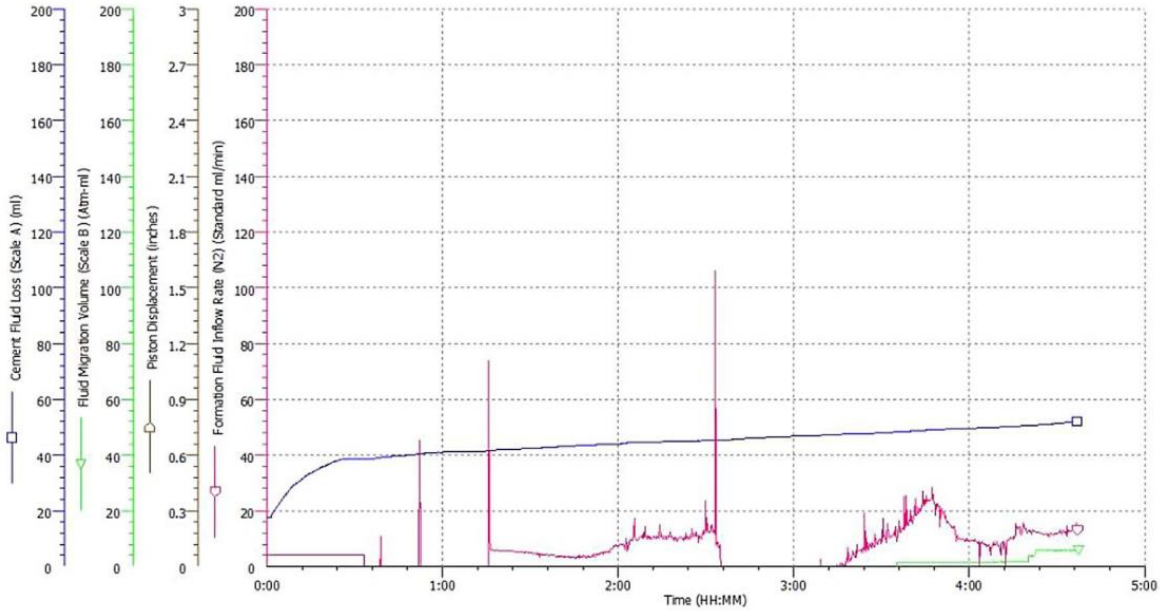

Table 7-1 summarized the FMA results for condition 1. It indicated that fluid migration decreased as nanosilica content increased from $0\%\ to\ 0.3\%$. So for $95\ PCF$ slurries, sample 1-D with 0.3% nanosilica showed the best performance in mitigating fluid migration.

Table 7-1 Effect of nanosilica on fluid migration. [88]

Condition	Density (PCF)	NS%	Migration (mL)
1-A	95	0	76
1-B	95	0.1	60
1-C	95	0.2	28
1-D	95	0.3	6
1-E	95	0.5	17

For condition 2 (FMA) Results:

sample 2-A, the FMA test showed $17\ mL$ of fluid migration. Notably, Figure 7-3 illustrates zero fluid migration for sample 2-B. Table 7-2 summarizes the FMA results for Condition 2. According to this data, the fluid migration for sample 2-B with 0.1% nanosilica was ideal/negligible. Comparing Tables 7-1 and 7-2 reveals that the fluid migration rate was lower for the 120 PCF slurries compared to the 95 PCF slurries. This could be attributed to the presence of an anti-gas migration additive in the 120 PCF slurry composition.

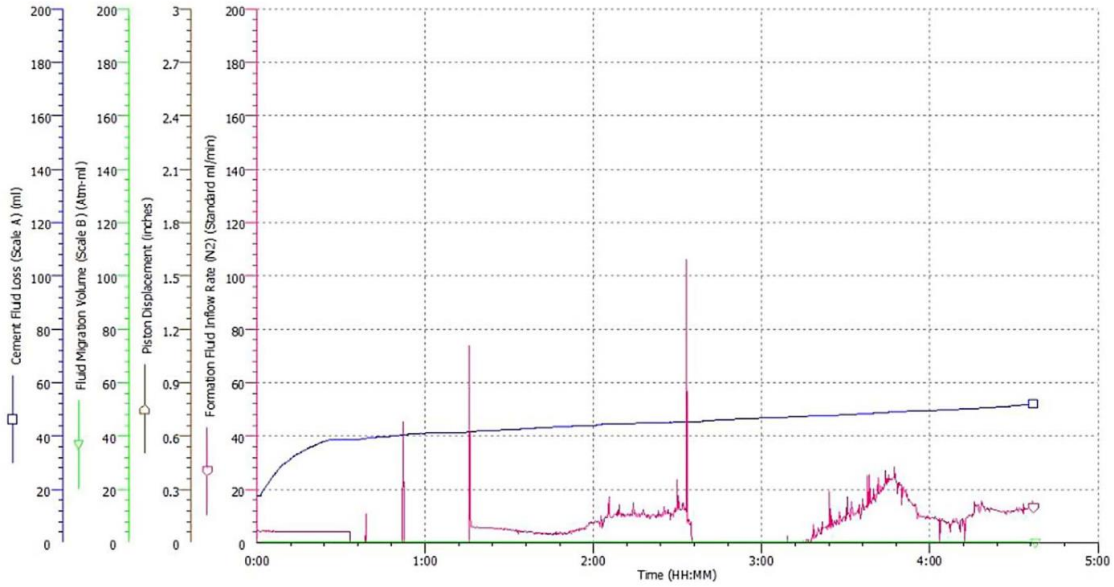

Figure 7-3 Fluid migration results (green) for 120 PCF with 0.1% nanoparticles [88]

Table 7-2 Effect of nanosilica on fluid migration for 120 PCF.[88]

Condition	Density (PCF)	NS%	Migration (mL)
2-A	120	0	41
2-B	120	0.1	0
2-C	120	0.2	21
2-D	120	0.3	N/A
2-E	120	0.5	N/A

Nanosilica decreased fluid migration in cement slurry, especially in optimum percentage of nanoparticles. For the higher density 120 PCF slurries, the 0.1% nanosilica addition (sample 2-B) provided the best performance in terms of minimizing fluid/gas migration based on the FMA tests conducted.

Comparing the two conditions, the 120 PCF had a higher success in the implementation in the industry and it can have higher success related to injecting super critical CO_2.

8 Conclusion:

This research can be summarized to:

- Carbon storage in abandoned oil wells must be optimized by reperforming a cementing job to enhance wellbore stability over injection span.
- Injection of super critical carbon can be fatal in the long and short term due to corrosive action of carbon dioxide by carbonation, bi-carbonation, and formation of carbonic acid.
- The comparison of experimental data and simulation proves the effect of exposure cement slurry to carbon dioxide in super critical form and dissolved in saline water.
- Additives are mandatory to prohibit the corrosive action on cement like pozzolanic material, nanoparticle, and ACA material.
- cementing job for relining casing into an abandoned wellbore can be risky and has to be optimized by good planning and operation.
- Nanoparticles can show a promising future on decreasing permeability and can be put into consideration for the next few years.

9 References:

[1] Erik B. Nelson, Dominique Guillot. (2006) Well Cementing second edition.

[2] GEFEI LIU. (2021) APPLIED WELL CEMENTING ENGINEERING

[3] Terry R. Smith. Cementing Displacement Practices Field Applications

[4] Azar, J. J., & Samuel, G. R. (2007). Drilling Engineering. Tusla: PennWell Corporation.

[5] Patil, R., & Deshpande, A. (2012). Use of Nanomaterials in Cementing Applicaions.

[6] Rocka, L. A., Falcao, J. L., Goncalves, C. J., Toledo, C., Lobato, K., Leal, S., & Lobato, H. m (2004). Fracture Pressure Gradient in Deepwater.

[7] McElfresh, P. M., & Boncan, V. C. (1982). Applications of Foam Cement.

[8] Allen, T. E., & Sands, F. L. (1993). Why Control Cement Slurry Density.

[9] Robert F. Mitchell Stefan Z. Miska. (2011) FUNDAMENTALS OF DRILLING nmENGINEERING

[10] Alexandre Lavrov, Malin Torsæter. Physics and Mechanics of Primary Well Cementing.

[11] Sabins, F. L., Tinsley, J. M., & Sutton, D. L. (1982). Transition Time of Cement Slurries Between the Fluid and Set States.

[12] Bruckdorfer, R., & Gleit, A. (1988). Static Fluid Loss Mode.

[13] Bannister, C., & Lawson, V. (1985). Role of Cement Fluid Loss in Wellbore Completion.

[14] Applied Well Cementing Engineering (2021) Gunnar DeBruijn, Sarah Misser Whitton

[15] Thiercelin, M., Dargaud, B., & Baret, J. (1998). Cement Design Based on Cement Mechanical Response.

[16] Reddy, B., Santra, A. K., McMechan, D. E., Gray, D. W., Brenneis, C., & Dunn, R. (2005). Cement Mechanical Property Measurements Under Wellbore Conditions.

[17] Myers, S. H., El Shaari, N. A., & Dillenbeck, R. L. (2005). A New Method to Evaluate Cement Systems Design Requirements for Cyclic Steam Wells.

[18] McDaniel, J., Watters, L., & Shadravan, A. (2014). Cement Sheath Durability: Increasing Cement Sheath Integrity to Reduce Gas Migration in the Marcellus Shale Play.

[19] Ramos, R. (1992). Thickening Time Measure to Simulate Cementing Operations on Deepwater Wells: Field Laboratory Validation.

[20] Shahriar, A. (2011). Investigation on Rheology of Oil Well Cement Slurries. PhD Thesis.

[21] National grid group PLC. Energy explained https://www.nationalgrid.com/stories/energy-explained/what-is-ccs-how-does-it-work

[22] Sarmiento, J.L. and Gruber, N. (2002) Sinks for anthropogenic carbon.

[23] NEDILJKA GAURINA-MEĐIMUREC, THE INFLUENCE OF CO_2 ON WELL CEMENT 2010

[24] Onan, D.D. (1984): Effects of Supercritical Carbon Dioxide on Well Cements.

[25] Kutchko, B.G., Strzisar, B.R., Dzombak, D.A., Lowry, G.V., Thaulow, N. (2007): Degradation of Well Cement by CO_2 under Geologic Sequestration Conditions.

[26] Lesti, M., Tiemeyer, C., & Plank, J. (2013). CO_2 stability of Portland cement based well cementing systems for use on carbon capture & storage (CCS) wells.

[27] A. Duguid. An estimate of the time to degrade the cement sheath in a well exposed to carbonated brine (2009)

[28] D.D. Onan Effects of supercritical carbon dioxide on well cements, (1984)

[29] Carey, J.W., Wigand, M., Chipera, S.J., WoldeGabriel, G., Pawar, R., Lichtner, P.C., Wehner, S.C., Raines, M.A., Guthrie, G.D. (2007): Analysis and performance of oil well cement with 30 years of CO_2 exposure from the SACROG Unit.

[30] Sweatman, R.E., Santra, A., Kulakofsky, D.S., Calvert, D.G.J. (2009): Effective Zonal Isolation for CO_2 Sequestration Weels.

[31] Carroll, Susan & Carey, Bill & Dzombak, David & Huerta, Nicolas & Li, Li & Richard, Tom & Um, Wooyong & Walsh, Stuart & Zhang, Liwei. (2016). Review: Role of chemistry, mechanics, and transport on well integrity in CO_2 storage environments.

[32] Santra, A., Reddy, B.R., Liang, F., Fitzgeralg, R. (2009): Reaction of CO_2 with Portland cement at Downhole Conditions and the Role of Pozzolanic Supplements.

[33] Rabia, H. (2002) Well Engineering & Construction.

[34] Gunnar DeBruijn and Sarah Misser Whitton, APPLIED WELL CEMENTING ENGINEERING

Chapter 5
[35] Ron Sweatman et al. IADC Drilling Manual 12th edition. (2015)
[36] Eric B, Joel F, Grace O (2016) Oil Well Cement Additives: A Review of the Common Types. Oil Gas Res 2
[37] Bett EK (2010) Geothermal Well Cementing Materials and Placement techniques
[38] Cements and Materials for Well Cementing. API SPECIFICATION 10A TWENTY-FIFTH EDITION, MARCH 2019
[39] Sugama, T.: Advanced Cements for Geothermal Wells, Energy Resources Division, Energy Science & Technology Department, Brookhaven National Laboratory, Upton, NY, 2006.
[40] Benge, G.: Improving Wellbore Seal Integrity in CO_2 Injection Wells, IADC/SPE Drilling Conference and Exhibition, IADC/SPE paper 119267, Amsterdam, 2009.
[41] Emissions from Oil and Gas Operations in Net Zero Transitions A World Energy Outlook Special Report on the Oil and Gas Industry and COP28. The European Commission also participates in the work of the IEA May 2023
[42] Steinour, H. H. (1959). Some effects of carbon dioxide on mortars and concrete-Discussion. Journal of the American Concrete Institute, 30, 905–907.
[43] Papadakis, V. G., Vayenas, C. G., & Fardis, M. N. (1989). A reaction engineering approach to the problem of concrete carbonation. AIChE Journal, 35(10), 1639–1650. https://doi.org/10.1002/aic.690351008
[44] Papadakis, V., Vayenas, C., & Fardis, M. (1991b). Fundamental modeling and experimental investigation of concrete carbonation. ACI Materials Journal, 88, 363–373.
[45] Papadakis, V. G., Vayenas, C. G., & Fardis, M. N. (1991a). Physical and chemical characteristics affecting the durability of concrete. Materials Journal, 88, 186–196. https://doi.org/10.14359/1993
[46] Jena Jeong, Hamidréza Ramézani, Vagelis G. Papadakis, Johan Colin & Laurent Izoret (2021): On CO2 sequestration in concrete aggregate via carbonation: simulation and experimental verification, European Journal of Environmental and Civil Engineering, DOI: 10.1080/19648189.2021.1928555
[47] Saillio, M., Bouny, V. B., Bertin, M., Vincent, J., & Lacaillerie, J.-B D. (2019, June 24–25). Quantification of bound CO2 in various carbonated [Paper presentation]. CO2STO2019, International Workshop CO2Storage in Concrete, Institut Franc¸ais des Sciences et Technologies des Transports, de L'Am enagement et des R eseaux - IFSTTAR, Champs-sur-Marne, France (pp. 251–261). https://hal. archives-ouvertes.fr/hal-03178179
[48] Zienkiewicz, O., & Taylor, R. (2005). The finite element method for solid and structural mechanics, The finite element method (6th ed.). Elsevier.
[49] Zienkiewicz, O. C., Taylor, R., & Zhu, J. (2005). The finite element method, its basis and fundamentals, The finite element method (6th ed.). Elsevier.
[50] Nunziato, J. W., & Cowin, S. C. (1979). A nonlinear theory of elastic materials with voids. Archive for Rational Mechanics and Analysis, 72(2), 175–201. https://doi.org/10.1007/BF00249363
[51] Cowin, J. W. (1983). Nunziato, Linear elastic materials with voids. Journal of Elasticity 13, 30125–147. https://doi.org/10.1007/BF00041230.
[52] Cowin, S. C. (1985). The viscoelastic behavior of linear elastic materials with voids. Journal of Elasticity, 15(2), 185–191. https://doi.org/10.1007/BF00041992
[53] Cowin, S. C., & Nunziato, J. W. (1983). Linear elastic materials with voids. Journal of Elasticity, 13(2), 125–147. https://doi.org/10.1007/BF00041230
[54] Markov, K. Z. (1998). On the cluster bounds for the effective properties of microcracked solids. Journal of the Mechanics and Physics of Solids, 46(2), 357–388. https://doi.org/10.1016/S0022-5096(97)00063-X
[55] Iovane, G., & Nasedkin, A. (2005). Finite element analysis of static problems for elastic media with voids. Computers & Structures 84(1–2), 19–24.

https://doi.org/10.1016/j.compstruc.2005.09.002
[56] Ramezani, H., & Jeong, J. (2011). Environmentally motivated modeling of hygro-thermally induced stresses in the layered limestone masonry structures: Physical motivation and numerical modeling. Acta Mechanica, 220(1–4), 107–137. https://doi.org/10.1007/s00707-011-0463-5
[57] Ramezani, H., & Jeong, J. (2015). Non-linear elastic micro-dilatation theory: Matrix exponential function paradigm. International Journal of Solids and Structures, 67-68, 1–26. https://doi.org/10.1016/j.ijsolstr. 2015.02.008
[58] Ramezani, H., Jeong, J., Bhatia, S. K., & Papadakis, V. G. (2021). Assessment of CO2 adsorption capacity in Wollastonite using atomistic simulation. Journal of CO2 Utilization. https://doi.org/10.1016/j.jcou.2021. 101564
[59] Ramezani, H., Jeong, J., & Feng, Z.-Q. (2011). On parallel simulation of a new linear Cosserat elasticity model with grid framework model assumptions. Applied Mathematical Modelling, 35(10), 4738–4758. https://doi.org/10.1016/j.apm.2011.03.054
[60] Ramezani, H., Mounanga, P., Jeong, J., & Bouasker, M. (2013). Role of cement paste composition on the self induced stress in early-age mortars: Application of the cosserat size number. Cement and Concrete Composites, 39, 43–59. https://doi.org/10.1016/j.cemconcomp.2013.03.005
[61] Ramezani, H., Steeb, H., & Jeong, J. (2012). Analytical and numerical studies on penalized micro-dilatation (PMD) theory: Macro-micro link concept. European Journal of Mechanics - A/Solids, 34, 130–148. https:// doi.org/10.1016/j.euromechsol.2011.11.002
[62] Dinh, T. X., Jeong, J., Ram ezani, H., & Feng, Z.-Q. (2011). Chemo-micro-dilatation modeling of carbonation shrinkage phenomenon of the porous mortars. Advanced Materials Research, 261–263, 680–684. https:// doi.org/10.4028/www.scientific.net/AMR.261-263.680
[63] Krunoslav Sedić and Nediljka Gaurina-Međimurec. CARBON DIOXIDE UNDERGROUND STORAGE AND ITS INFLUENCE ON WELL CEMENT 2016
[64] Živković H., Leonard N., Sentić M., Mudrić D., Hudek J., Devedija B., Turković D., Novosel D., Krš E., Habijanec Ž., Vukšinić D., Brešić M., Aračić A. & Škrnjug M: Mining project of hydrocarbon production on Zutica oil field.
[65] Živković H., Leonard N., Sentić M., Mudrić D., Hudek J., Devedija B., Turković D., Novosel D., Krš E., Habijanec Ž., Vukšinić D., Brešić M., Aračić A. & Škrnjug M: Mining project of hydrocarbon production on Ivanic oil field.
[66] Novosel, D. (2010): Učinak ugljičnog dioksida u tercijarnoj fazi iskorištavanja naftnih ležišta polja Ivanić, Nafta, 61 (2010).
[67] Adams, N. J. & Charrier, T. (1985): Drilling Engineering – A Complete Well Planning Approach, Penn Well Publishing Company, Tulsa, Oklahoma, 1985.
[68] Hudek J., Habijanec Ž., Kosovec Z. & Majder D.: Simplified mining project of major equipment workover on Zutica-111 well (Zu-111, Zagreb, 2012.
[69] Habjanec G., Maskalan S., Habijanec Ž., Mudrić D., Ljepović-Olujić V., Fiak D., Račić M., Pintar A. & Jukić L.: Simplified mining project of major equipment workover on Ivanic-70 well (Iva-70), Zagreb, 2013.
[70] Bai, M., Sun, J., Song, K., Li, L., Qiao, Z., 2015. Well completion and integrity evaluation for CO2 injection wells. Renew. Sustain. Energy Rev. 45, 556–564.
[71] Ilesanmi, O.R., Hilal, B., Gill, S., Brandl, A., 2013. Long term wellbore isolation in a corrosive environment, SPE/IADC Middle East Drilling Technology Conference & Exhibition. Society of Petroleum Engineers, Dubai.
[72] Yuanguang Yang , Bin Yuan, Yongqing Wang, Shipei Zhang, Liang Zhu. Carbonation resistance cement for CO2 storage and injection wells 2016
[73] Brandl, A., Cutler, J., Seholm, A., Sansil, M., Braun, G., 2010. Cementing Solutions for Corrosive Well Environments. 2010
[74] Barlet-Gouedard, V., Rimmele, G., Goffe, B., Porcherie, O., 2007. Well technologies for CO2

geological storage: CO2-resistant cement.
[75] Li, Z.Y., Guo, X.Y., Han, L., Luo, P.Y., 2007. Improvement of latex on mechanical deformation capability of cement sheath under triaxial loading condition.
[76] Yuanhua, L., Dajiang, Z., Dezhi, Z., Yuanguang, Y., Taihe, S., Kuanhai, D., Chengqiang, R., Deping, Z., Feng, W., 2013. Experimental studies on corrosion of cement in CO2 injection wells under supercritical conditions.
[77] Yang, Y., Yuan, B., Sun, Q., Tang, X., Yingquan, X., 2015. Mechanical properties of EVA-modified cement for underground gas storage.
[78] Gabriela Gonçalves, Dias Ponzi, Victor Hugo Jacks Mendes dos Santos, Renan Bordulis Martel, Darlan Pontin, Amanda Sofia de Guimaraesae Stepanha, Marta Kerber Schütz, Sonia C. Menezes, Sandra M.O. Einloft , Felipe Dalla Vecchia. Basalt powder as a supplementary cementitious material in cement paste for CCS wells: chemical and mechanical resistance of cement formulations for CO2 geological storage sites
[79] Schütz, M.K., Baldissera, A.F., Coteskvisk, P.M., Vecchia, F.D., Menezes, S.C., Miranda, C. R., Einloft, S., 2018. Chemical degradation of reinforced epoxy-cement composites under CO2-rich environments. Polym. Compos. 39, E2234–E2244. https://doi.org/ 10.1002/pc.24589.
[80] Ghafari, E., Feys, D., Khayat, K., 2016. Feasibility of using natural SCMs in concrete for infrastructure applications. Constr. Build. Mater. 127, 724–732. https://doi.org/ 10.1016/j.conbuildmat.2016.10.070.
[81] Tiong, M., Gholami, R., Rahman, M.E., 2019. Cement degradation in CO2 storage sites: a review on potential applications of nanomaterials. J. Pet. Explor. Prod. Technol. 9, 329–340. https://doi.org/10.1007/s13202-018-0490-z.
[82] Teodoriu, C., Bello, O., 2020. A review of cement testing apparatus and methods under CO2 environment and their impact on well integrity prediction – Where do we stand? J. Pet. Sci. Eng. 187, 106736 https://doi.org/10.1016/j.petrol.2019.106736.
[83] El-Didamony, H., Helmy, I.M., Osman, R.M., Habboud, A.M., 2015. Basalt as Pozzolana and Filler in Ordinary Portland Cement. Am. J. Eng. Appl. Sci. 8, 263–274. https:// doi.org/10.3844/ajeassp.2015.263.274.
[84] Dobiszewska, M., Beycioglu, ˘ A., 2017. Investigating the Influence of Waste Basalt Powder on Selected Properties of Cement Paste and Mortar. IOP Conf. Ser. Mater. Sci. Eng. 245, 022027 https://doi.org/10.1088/1757-899X/245/2/022027.
[85] Jadid, K.M., Okandan (Supervisor), E., 2011. Chemical alteration of oil well cement with basalt additive during carbon storage application. Master Thesis. Middle East Technical University.
[86] Raverdy, M., Brivot, F., Paillere, A.M., Dron, R., 1980. Appreciation de l'activite pouzzolanique de constituents secondaires. In: Proceedings of 7e Congr´es International de La Chimie Des Ciments.
[87] Bertos, M.F., Simons, S.J.R., Hills, C.D., Carey, P.J., 2004. A review of accelerated carbonation technology in the treatment of cement-based materials and sequestration of CO2. J. Hazard. Mater. 112, 193–205. https://doi.org/10.1016/j. jhazmat.2004.04.019.
[88]Mahmoud Bayanak, Soroush Zarinabadi, Khalil Shahbazi , and Alireza Azimi. Reduction of fluid migration in well cement slurry using nanoparticles
[89] Moritis G. (2008) SWP advances CO2 sequestration ECBM EOR demos, Oil Gas J. 106, 37, 60–63.
[90] Dean G.D., Brennen M.A. (1992) A unique laboratory gas flow model reveals insight to predict gas migration in cement, in: SPE Western Regional Meeting, Bakersfield, California 30 March–1 April 1992. SPE-24049-MS. doi: 10.2118/24049-MS.
[91] Ahmed S., Ezeakacha C.P., Salehi S. (2018) Improvement in cement sealing properties and integrity using conductive carbon nano materials: From strength to thickening time, in: SPE Annual Technical Conference and Exhibition, Dallas, Texas, USA, 24–26 September 2018. SPE-191709-MS, doi: 10.2118/191709-MS.
[92] Abbas G., Irawan S., Kumar S., Kalwar S.A. (2014) Experimental study of gas migration

prevention through cement slurry using hydroxypropylmethylcellulose, in: IADC/SPE Asia Pacific Drilling Technology Conference, Bangkok, Thailand, 25–27 August 2014. SPE-170538-MS. https://doi-org.ezproxy.lib.ou.edu/10.2118/170538-MS
[93] King G.E., King D.E. (2013) Environmental risk arising from well-construction failure-differences between barrier and well failure and estimates of failure frequency across common well types, locations, and well age, SPE Prod. Oper. 28, 4, 323–344. SPE-166142-PA. doi: 10.2118/166142-PA.
[94] Griffin T., Spangle L., Nelson E. (1979) New expanding cement promotes better bonding, Oil Gas J. 77, 26, 143.
[95] Němeček J., Li L., Xi Y. (2017) Electrokinetic nanoparticle injection for remediating leaks in oil well Cement, Constr. Build. Mater. 156, 63–72. doi: 10.1016/j.conbuildmat.2017. 08.152.
[96] Goboncan V.C., Dillenbeck R.L. (2003) Real-time cement expansion/shrinkage testing under downhole condition for enhanced annular isolation, in: SPE/IADC Drilling Conference. doi: 10.2118/79911-ms.
[97] Mata C., Calubayan A. (2016) Use of hollow glass spheres in lightweight cements – selection criteria, in: SPE – Asia Pacific Oil & Gas Conference and Exhibition. doi: 10.2118/ 82399-ms.
[98] Al-Yami A.S., Al-Humaidi A.S. (2016) High density cement formulation to prevent gas migration problems. Google Patents 2016. doi: 10.2118/187700-MS.
[99] Al-Yami A.S. (2015) An Innovative cement formula to mitigate gas migration problems in deep gas wells: Lab studies and field cases, in: SPE Kuwait Oil & Gas Show and Conference, Mishref, Kuwait, 11–14 October 2015. doi: 10.2118/175194-MS.
[100] Pour M.M., Moghadasi J. (2007) New cement formulation that solves gas migration problems in Iranian South Pars field condition, in: SPE Middle East Oil and Gas Show and Conference, Society of Petroleum Engineers. doi: 10.2523/ 105663-MS.
[101] Lackey G., Rajaram H., Sherwood O.A., Burke T.L., Ryan J.N. (2017) Surface casing pressure as an indicator of well integrity loss and stray gas migration in the Wattenberg Field Colorado, Environ. Sci. Technol. 51, 6, 3567–3574.
[102] Nelson E.B., Guillot D. (2006) Well cementing, 2nd edn., Schlumberger, Sugar Land, Texas, USA.